



Review Article

Computer vision in smart agriculture and precision farming: Techniques and applications

Sumaira Ghazal ^a, Arslan Munir ^{b,*}, Waqar S. Qureshi ^c

^a Department of Computer Science, Kansas State University, 66506 Manhattan, KS, USA

^b Department of Electrical Engineering and Computer Science, Florida Atlantic University, 33431 Boca Raton, FL, USA

^c School of Computer Science, University of Galway, H91 TK33 Galway, Ireland

ARTICLE INFO

Article history:

Received 10 September 2023

Received in revised form 8 June 2024

Accepted 19 June 2024

Available online 25 June 2024

Keywords:

Digital agriculture

Computer vision

Smart agriculture

Image analysis

Vision-guided intelligent systems

ABSTRACT

The transformation of age-old farming practices through the integration of digitization and automation has sparked a revolution in agriculture that is driven by cutting-edge computer vision and artificial intelligence (AI) technologies. This transformation not only promises increased productivity and economic growth, but also has the potential to address important global issues such as food security and sustainability. This survey paper aims to provide a holistic understanding of the integration of vision-based intelligent systems in various aspects of precision agriculture. By providing a detailed discussion on key areas of digital life cycle of crops, this survey contributes to a deeper understanding of the complexities associated with the implementation of vision-guided intelligent systems in challenging agricultural environments. The focus of this survey is to explore widely used imaging and image analysis techniques being utilized for precision farming tasks. This paper first discusses various salient crop metrics used in digital agriculture. Then this paper illustrates the usage of imaging and computer vision techniques in various phases of digital life cycle of crops in precision agriculture, such as image acquisition, image stitching and photogrammetry, image analysis, decision making, treatment, and planning. After establishing a thorough understanding of related terms and techniques involved in the implementation of vision-based intelligent systems for precision agriculture, the survey concludes by outlining the challenges associated with implementing generalized computer vision models for real-time deployment of fully autonomous farms.

© 2024 The Authors. Publishing services by Elsevier B.V. on behalf of KeAi Communications Co., Ltd. This is an open access article under the CC BY-NC-ND license (<http://creativecommons.org/licenses/by-nc-nd/4.0/>).

1. Introduction

Vision-based intelligent systems have made way to practically every aspect of modern human life. These systems combine computer vision, artificial intelligence (AI), and machine learning technologies and allow machines to mimic human visual and cognitive abilities to make informed decisions about the task at hand. Computer vision technology is used to process and interpret visual information from the surrounding environment while the artificial intelligence (AI) technologies along with machine learning algorithms are used for recognizing patterns and predicting actions. These intelligent systems improve performance through learning over time. Automated vision-based systems have revolutionized every industry since the late 20th century. Research on machines with the ability to interpret visual information started during 1950s. An example of one of the earliest intelligent machines is Shakey (DARPA, 2024), a groundbreaking robot developed at Stanford Research

Institute in the late 1960s. 1970s witnessed the origination of optical character recognition technology. In 1980s and 1990s, focus shifted on the application of machine learning techniques in the development of vision-based intelligent systems. However, these initial systems remained comparatively elementary, based mostly on rule-based approaches (Edem Gold, 2023). With the advancement in powerful computing resources and computer vision techniques like object recognition and image segmentation in 2000s, and advent of deep neural networks in 2010s, performance of vision-based systems has increased significantly. The intersection of the vision-based intelligent systems and robotics domains give rise to novel smart machines that have the ability to perceive and interact with their environment and perform tasks in a manner similar to humans.

There are numerous challenges for implementing intelligent systems in agricultural sector considering the widely increasing world population, declining arable land, and shortage of labor force. Pest damage

* Corresponding author.

E-mail addresses: sghazal@ksu.edu (S. Ghazal), arslanm@fau.edu (A. Munir), waqarshahid.qureshi@universityofgalway.ie (W.S. Qureshi).

as well as complex and unpredictable environment also add to the challenges faced by farmers (Marks, 2023). Farmers need a variety of information to make necessary decisions about the crops. Traditionally, this is done by physically monitoring the plants by the farmers at various times of crop development making it a cumbersome process requiring great focus and expertise. Subjective process of crop data extraction can be standardized by replacing manual extraction by automated systems based on latest AI and computer vision technologies. Focus of the present day research in agricultural sector is the development of intelligent and automated vision-guided systems that can replace manual processes and are more precise and accurate and free from human error factors. A vision-guided intelligent system must be able to gather relevant information without human intervention consequently reducing labor cost. With the data about current growth stage of the crop, such a system can be helpful for the timely and precise application of fertilizers and targeted spraying of insecticides/herbicides for better plant health and quality of produce thus increasing environmental sustainability and food security. A vision-guided intelligent system will also help in tracking the growth stages of the crop and making timely decision about harvest for better yield.

This article presents a comprehensive overview of the digital life cycle of crops in precision agriculture. We address various stages of digital agriculture, including image acquisition, image stitching, image analysis, decision-making with machine learning, and crop treatment and farm planning. Our motivation stemmed from the observation that current literature often focuses on individual areas without providing a holistic view or detailed explanation of the entire process involved in the implementation of digital agriculture. Many surveys concentrate on literature reviews within specific areas. For example, (Liu and Wang, 2021; Shafik et al., 2023; Jackulin and Murugavalli, 2022; Ouhami et al., 2021; Chithambarathanu and Jeyakumar, 2023) summarize studies on pest and disease detection in crops. Sethy et al. (2022) and Lu et al. (2020) discuss hyperspectral imaging applications in agriculture. Luo et al. (2023) specifically focus on the application of computer vision and deep learning in the context of Controlled Environment Agriculture (CEA) where CEA is a form of agriculture that involves growing plants within a controlled environment like greenhouses and plant factories Wagner et al. (2021). While the review by (Patrício and Rieder, 2018) explore key areas such as disease detection, grain quality assessment, and phenotyping, their work is limited to exploring the literature review for selective grain crops including maize, rice, wheat, soybean, and barley. Tian et al. (2020) have conducted a literature review focusing on key application areas of precision agriculture, such as growth monitoring, disease control, harvesting, quality testing, and farm management, in the context of agricultural automation. Although they discuss image analysis and decision-making techniques in these areas, their review lacks a comprehensive overview of the digital agriculture pipeline, including its various stages. The approach of Kakani et al. (2020) highlights the significance of computer vision and AI in the agriculture and food industry. While the authors discuss challenges, recommendations, and implications of incorporating these technologies into farming, global policies, and investments for sustainable food production, their main focus is to examine various scenarios and use cases where machine learning, machine vision, and deep learning are applied globally, particularly focusing on their sustainability aspects. This survey aims to bridge the gap in current literature by offering a thorough exploration of the complete digital agriculture pipeline, highlighting challenges in each stage/area of the pipeline. Additionally, we discuss widely used crop metrics in digital agriculture. Unlike most surveys that concentrate on specific applications of computer vision in certain areas, our paper provides a comprehensive understanding of the digital life cycle of crops in precision agriculture. We aim for our survey to provide researchers with a concise overview of the digital agriculture pipeline, sparking inspiration for new research and development in relevant areas.

Fig. 1 gives a detailed pipeline of the life cycle of crops in digital agriculture. The pipeline starts with image acquisition, employing various means for capturing the crop view, thereby replicating and enhancing the farmer's vision. These images are then processed using computer vision techniques and may either be directly used for analysis and data extraction or used for generating panoramic views for digital mapping and analyzing afterwards. After data and information extraction, various machine learning and AI techniques are used to generate predictions and estimates relevant to the problem at hand. These analyzed results and estimations are then utilized by farmers to formulate effective plans and treatments for crops aimed at maximizing their yield. This survey discusses the digital life cycle of crops, from image acquisition to planning and decision-making, along with relevant state-of-the-art methods of implementing the vision-guided intelligent systems. Focus of this survey is to compare the methodologies adopted for problem areas related to precision agriculture. Following research questions were kept in mind while performing review of articles: Q1: What type of imaging technology was employed by the researchers? Q2: What techniques were used for crop data extraction and comparison? Q3: What were the significant outcomes and results of these studies? The research articles were gathered from various Scopus-indexed peer-reviewed journals and conference proceedings. Considering the fast pace of technological advancements, only research articles from the last decade that is, after 2013 were considered. All the selected articles are summarized and presented in Sections 3 to 8. Before delving into a detailed review of existing research on vision-based intelligent systems in precision agriculture, it is essential to introduce certain key crop matrices that are widely used in precision agriculture research. Understanding these matrices is crucial to grasp the variation of their usage in the related research. These crop metrics are described in Section 2. Overview of main sections and subtopics covered in the survey are presented in Fig. 2.

2. Crop metrics for digital agriculture

Crop metrics are the statistics used to measure or quantify crop health, characteristics, and properties. A key subset of these metrics are Vegetation Indices (VIs), which are spectral imaging transformations used for estimating multiple crop/vegetation properties. VIs are derived by combining two or more spectral bands of electromagnetic spectrum that enhance vegetation properties and enable credible spatial and temporal inter-comparisons of terrestrial photosynthetic activity, variations in canopy structure, and various plant characteristics (Huete et al., 2002). This section provides an overview of selected crop metrics and VIs commonly applied in precision agriculture, aiming to clarify any discrepancies in their portrayal found in the literature. Table 1 provides a summary of VIs along with their applications in smart agriculture and precision farming. While the list presented here is not exhaustive, interested readers can find more information in (IDB, 2023).

2.1. Normalized difference vegetative index (NDVI)

NDVI is the most commonly used vegetation health index. It is used to measure the amount and vigor of vegetation on the land surface, and is useful to quantify vegetation greenness, vegetation density, and yield. NDVI can also be used to evaluate changes in plant health. NDVI spatial composite images are helpful in distinguishing green vegetation from bare soil (USDA, 2023). The formula for calculating NDVI is given by the Eq. (1) (Huete et al., 2011).

$$NDVI = (NIR - R)/(NIR + R) \quad (1)$$

where NIR = 800 nm and R = 670 nm. The range of NDVI values is from −1.0 to 1.0, where negative values indicate clouds and water, positive

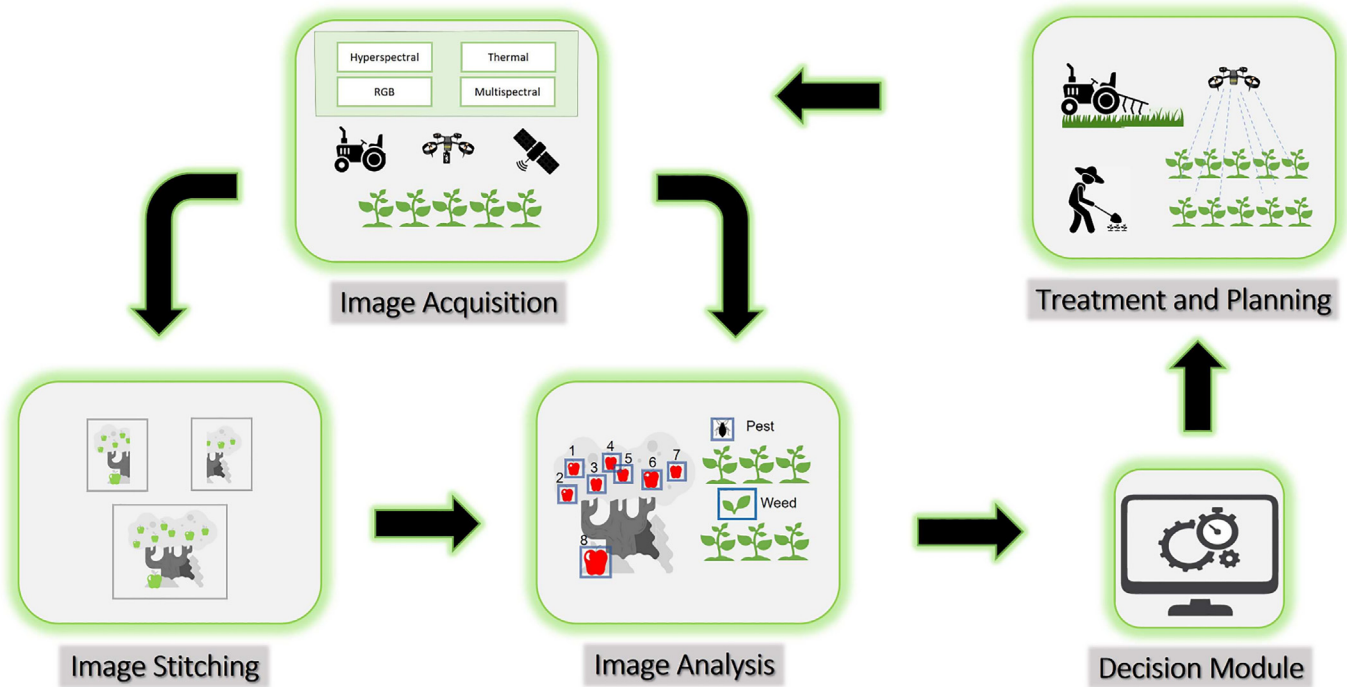


Fig. 1. Digital life cycle of crops in precision agriculture.

values near zero signify bare soil, higher positive values from 0.1 to 0.5 represent sparse vegetation, and even higher positive values from 0.6 to 1 represent dense green vegetation (USDA, 2023).

2.2. Normalized difference water index (NDWI)

It is used to detect water stress in plants (Cai Gao, 1996). The formula for calculating NDWI is given by Eq. (2).

$$NDWI = (NIR - SWIR) / (NIR + SWIR) \quad (2)$$

where NIR = 860 nm and SWIR = 1240 nm. The range of NDWI values is from -1.0 to 1.0 where higher values correspond to higher water content in vegetation. NDWI value will decrease for an increase in water stress (NDWI – EUROPE, P.F.S, 2011).

2.3. Crop water stress index (CWSI)

It is an indicator of water stress in crops. The temperature of plant leaf is determined by the extent of soil moisture and ambient conditions. Transpiration is the cause of drop in canopy temperature. The concept behind CWSI is that the decline in soil moisture causes a decline in transpiration hence increasing the canopy temperature. By measuring the relative transpiration rate of the plant using CWSI, water stress can be estimated. The formula (Agam et al., 2013) for calculating CWSI is given by Eq. (3).

$$CWSI = (T_c - T_w) / (T_d - T_w) \quad (3)$$

where T_c refers to the average crown temperature of a plant, T_w is the temperature of a non stressed leaf while T_d is the temperature of a stressed leaf. The range of CWSI is 0 to 1 where higher value indicates a low water stress level.

2.4. Green normalized difference vegetation index (GNDVI)

It is similar to NDVI but uses green band instead of red. It is more sensitive to photosynthetic activity and is commonly used for water and nitrogen content measurement. The formula (Gitelson et al., 1996) is given in Eq. (4).

$$GNDVI = (NIR - G) / (NIR + G) \quad (4)$$

where NIR = (780 nm to 1400 nm) and G = (540 nm to 570 nm) is the green band of electromagnetic spectrum. The range of GNDVI values range from -1.0 to 1.0, where values between -1 to 0 signify water and bare soil, while values between 0 and 1 represent sparse to dense vegetation.

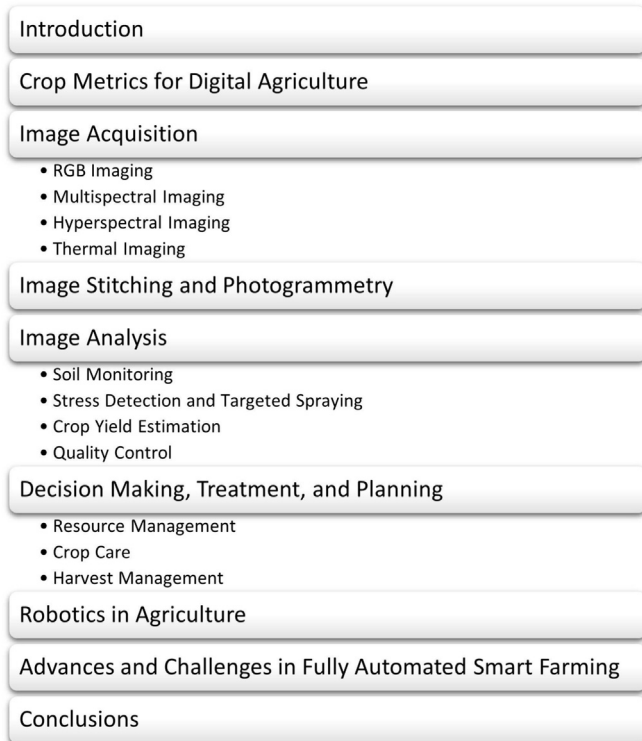


Fig. 2. Overview of main sections and subtopics in the survey.

Table 1
Vegetation Indices.

VI with Formula	*Spectral Bands (nm)	Applications	Reference
NDVI = (NIR-R)/(NIR + R)	R[655–665] & NIR[835–865]; R[670] & NIR[800]; R[575–675] & NIR[810–890]; R[615–685] & NIR[755–805]; R[640–680] & NIR[770–810]	Vegetation land cover mapping; Yield estimation; Vegetation density estimation; Nitrogen & water stress; Biotic stress detection	(Essaadia et al., 2022); (Gong et al., 2018); (Sabah et al., 2022); (Maresma et al., 2016); (Marin et al., 2021)
EVI = 2.5 * (NIR-R)/(NIR + 6*R + 7.5*B + 1)	R[670], NIR[800] & B[490]; R[670], NIR[800] & B[450]	Yield estimation; Biotic stress detection	(Gong et al., 2018); (Zhao et al., 2020a)
RDVI = (NIR-R)/(NIR + R) ^{0.5}	R[670] & NIR[800]; R[670] & NIR[800]	Yield estimation; Nitrogen & water stress detection	(Gong et al., 2018); (Rubo and Zinkernagel, 2022)
TVI = 0.5*[120(NIR-G)-200(R-G)]	R[670], NIR[800] & G[550]; R[650–680], NIR[780–890] & G[560–600]	Yield estimation; Biotic stress and yield estimation	(Gong et al., 2018); (Cao et al., 2015)
SAVI = (NIR-R)/(NIR + R + 0.5)*(1 + 0.5)	R[670] & NIR[800]; R[575–675] & NIR[810–890]; R[660] & NIR[790]; R[630–690] & NIR[760–900]	Yield estimation; Vegetation density estimation; Nitrogen & water stress detection; Biotic stress detection	(Gong et al., 2018); (Sabah et al., 2022); (Mwinuka et al., 2022); (Théau et al., 2020)
OSAVI = (NIR-R)/(NIR + R + 0.16)	R[575–675] & NIR[810–890]; R[660] & NIR[790]; R[717] & NIR[840]; R[640–680] & NIR[770–810]	Vegetation density estimation; Nitrogen & water stress detection; Yield estimation; Biotic stress detection	(Sabah et al., 2022); (Mwinuka et al., 2022); (Danilevicz et al., 2021); (Marin et al., 2021)
WDRVI = (0.1*NIR-R)/(0.1*NIR + R)	R[615–685] & NIR[755–805]	Nitrogen & water stress detection and yield estimation	(Maresma et al., 2016)
GNDVI = (NIR-G)/(NIR + G)	G[550] & NIR[790]; G[560] & NIR[840]; G[520–600] & NIR[760–900]	Nitrogen & water stress detection; Yield estimation; Biotic stress detection	(Mwinuka et al., 2022); (Danilevicz et al., 2021); (Théau et al., 2020)
NDRE = (NIR-RE)/(NIR + RE)	RE[735] & NIR[790]; RE[712–722] & NIR[820–860]	Nitrogen & water stress detection; Biotic stress detection	(Mwinuka et al., 2022); (Shahi, 2023)
CWSI = (T _c -T _w)/(T _d -T _w)	–	Water stress detection	(Gonzalez-dugo et al., 2013; Espinoza et al., 2017)
LAI = A _L /A _G	–	Yield estimation; Biotic stress detection	(Bascon et al., 2022); (Shahi, 2023)
NDWI = (NIR-SWIR)/(NIR + SWIR)	NIR[750–1300] & SWIR[1300–2500]	Biotic stress detection	(Yu et al., 2018)
PSRI = (R-G)/RE	R[630–690], G[545–575 nm] & RE[712–722]	Biotic stress detection	(Shahi, 2023)
DSI = $\sum (CF \cdot S)/(TP \cdot I_{max}) \cdot 100$	–	Disease severity detection	(Zhao et al., 2020a); (Fenu and Mallocci, 2021)

T_c - average crown temperature of a plant, T_w - temperature of a non-stressed leaf, T_d - temperature of a stressed leaf; A_L - Leaf area of a plant and A_G - Ground area occupied by plant; CF - class frequency, S - score of rating class, TP - total number of observations, I_{max} - maximal disease index the rating scale.

* This column gives the wavelengths of the spectral bands chosen by various researchers (as cited in corresponding reference column) for a given vegetation index.

2.5. Enhanced vegetation index (EVI)

It is an optimized vegetation index that takes into account atmospheric background, soil conditions and canopy structure and is developed for correction of NDVI values specifically for dense vegetation. The EVI is useful in measuring drought related stress (Integrated Drought Management Programme, 2024). Its range varies between −1.0 to 1.0 where higher values are associated with healthy vegetation. The formula (IDB, 2023) for calculating EVI is given in Eq. (5).

$$EVI = 2.5 \times (NIR - R)/(NIR + 6 \times R + 7.5 \times B + 1) \quad (5)$$

where B = (420 nm to 480 nm), R = (640 nm to 760 nm) and NIR = (780 nm to 1400 nm) (IDB, 2023).

2.6. Leaf area index (LAI)

It is used to measure crop growth and canopy structure. It is calculated as half the area (one-sided area) of green leaves per unit ground surface area. LAI has a highly variable range with LAI of less than 1 for some desert ecosystems and LAI around 9 for dense tropical rainforests (Campbell, n.d.).

$$LAI = A_L/A_G \quad (6)$$

where A_L denotes the leaf area of a plant and A_G denotes the ground area occupied by the plant.

2.7. Normalized difference red edge index (NDRE)

NDRE is used to measure the plant chlorophyll content. It is used to differentiate between healthy and stressed vegetation. The formula (Barnes et al., 2000) is given in Eq. (7).

$$NDRE = (NIR - RE)/(NIR + RE) \quad (7)$$

where NIR = 790 nm and RE = 720 nm. NDRE values range between −1.0 to 1.0. Highest values of NDRE correspond to healthy and middle range values correspond to unhealthy vegetation. Bare soil has the lowest values.

2.8. Soil adjusted vegetation index (SAVI)

It corrects the NDVI value by using a soil brightness correction factor for low vegetation areas. The formula (Huete, 1988) is given in Eq. (8).

$$SAVI = (NIR - R)/(NIR + R + L) \times (1 + L) \quad (8)$$

where NIR = 800 nm, R = 670 nm and L = 0.5 for most land covers. For L = 0, SAVI = NDVI. SAVI values lie between range −1.0 to 1.0. Higher SAVI values correspond to denser vegetation while lower values correspond to little or no vegetation similar to NDVI.

2.9. Optimized soil adjusted vegetation index (OSAVI)

It refers to an optimized version of SAVI (Rondeaux, 1996). The formula is given in Eq. (9).

$$OSAVI = (NIR - R)/(NIR + R + 0.16) \quad (9)$$

where NIR = 800 nm and R = 670 nm. OSAVI values lie between range −1.0 to 1.0. Higher OSAVI values correspond to denser while lower values correspond to little vegetation.

2.10. Plant senescence reflectance index (PSRI)

It is used for plant stress detection and yield estimation. The formula is given by Eq. (10) in terms of reflectance values (Merzlyak et al., 1999).

$$PSRI = (R - G)/RE \quad (10)$$

where $R = 678$ nm, $G = 500$ nm and RE (Red Edge) = 750 nm. The range of values for PSRI lies between -1.0 to 1.0 . Higher values of PSRI indicate the ripening of fruit and increased canopy senescence and stress.

2.11. Wide dynamic range vegetation index (WDRVI)

It is similar to NDVI but more accurate for measuring canopy differences in high density vegetation. The formula is given in Eq. (11).

$$WDRVI = (a \times NIR - R)/(a \times NIR + R) \quad (11)$$

where $R = (580$ nm to 680 nm), $NIR = (725$ nm to 1000 nm) and a is a weighting coefficient that lies in range 0.1 to 0.2 (Gitelson, 2004). The range of values lies between -1.0 to 1.0 . If weighting coefficient $a = 1$ then $WDRVI = NDVI$.

2.12. Renormalized difference vegetation index (RDVI)

It is used for detection of healthy vegetation. It is an improvement in NDVI in order to linearize the relationship with LAI. The formula (Roujean and Breon, 1995) is given in Eq. (12).

$$RDVI = (NIR - R)/(NIR + R)^{0.5} \quad (12)$$

where $NIR = 850$ nm and $R = 650$ nm. The range of values lies between -1.0 to 1.0 .

2.13. Triangular vegetation index (TVI)

It measures the area of hypothetical triangle made by green peak, red minimum reflectance and near infrared shoulder (Haboudane et al., 2004). It is sensitive to leaf chlorophyll content and can be used for nitrogen stress detection in plants. The formula is given in the Eq. (13).

$$TVI = 0.5 \times [120 \times (NIR - G) - 200 \times (R - G)] \quad (13)$$

where $NIR = 750$ nm, $G = 550$ nm and $R = 670$ nm. The range of values for TVI lies between -1 and 1 . Higher TVI values indicate healthy and dense vegetation while lower values may indicate stressed or sparse vegetation, or surfaces other than vegetation.

2.14. Disease severity index (DSI)

It is a percentage that is used to determine the severity level of disease in plants and is used with the data represented on a special ordinal scale. The classes are comprised of consecutive ranges of defined intervals that are based on the area percentage of disease symptoms. The formula (Chiang et al., 2017) is given in Eq. (14).

$$DSI = \sum(CF \times S)/(TP \times I_{max}) \times 100 \quad (14)$$

where CF is class frequency corresponding to the number of observations occurring in a class interval, S is the score of rating class on the ordinal scale, TP is the total number of observations, and I_{max} is the maximal disease index that is the highest numerical point on the rating scale. DSI values range from 0% (no disease) to 100% (maximal disease).

3. Image acquisition

Imaging technology in agriculture includes the use of ground sensing robots, aerial drone imaging and remote sensing using satellite imagery. With these image acquisition technologies, it is possible to

examine and monitor the crops in real time for better health assessment, yield estimation and determining the soil conditions leading to better quality produce and advanced planning. Core imaging technologies used in agricultural imaging include red, green and blue (RGB), multispectral hyperspectral, and thermal imaging as depicted in Fig. 3.

3.1. RGB imaging

A widely used imaging method is RGB imaging that uses the digital camera to capture visible light reflected from the objects to produce a digital image. Visible light falls in the 400 – 700 nm range of electromagnetic spectrum and includes red, blue and green bands of the electromagnetic spectrum. RGB imaging technique has been widely employed by the researchers for various precision agriculture applications. Liu (2022) used a high resolution CMOS sensor based RGB camera to capture soil sample images for soil water content detection. Azimi et al. (2021b) used CMOS digital single-lens reflex (SLR) camera for chickpea plant shoot imaging for water stress detection. Zhang et al. (2022) also used a digital SLR camera for disease detection in grapevine. Khan et al. (2021) attached an RGB camera to unmanned air vehicle (UAV) to get images of coriander field for spraying area recognition for weed control. Tagarakis et al. (2022) used an RGB depth camera mounted on an unmanned ground vehicle (UGV) for 3D reconstruction of a commercial walnut orchard. Lee et al. (2023) detected defected apples using a multi-camera system employing RGB imaging. Maheswari et al. (2022) performed tomato yield estimation using RGB imaging technology. The images were taken at night time to avoid illumination effects due to sunlight.

3.2. Multispectral imaging

Multispectral imaging collects a few discrete spectral bands, typically less than 10 , including RGB channels from visible spectrum, near and far infrared, and near ultraviolet bands of the electromagnetic spectrum. Multispectral imagery can be used for early identification of stresses in crops, enabling timely decisions to increase crop yield while minimizing the use of pesticides and fertilizers. Multispectral data can also be used for crop yield estimation by plant counting. Vegetation indices such as NDVI can be calculated to measure water content in plants. An example of multispectral imaging is the work of Adhikari et al. (2020), who developed a smartphone based imaging module for measuring plant nitrogen content using multispectral imaging technique. Another example that utilizes a UAV for obtaining the images of rice crop, is the work of Colorado et al. (2020). They used Parrot Sequoia multispectral sensor for leaf nitrogen content estimation. Singh and Gaurav (2023) used multispectral satellite imagery for soil surface moisture content estimation. Fraccaro et al. (2022) used a combination of RGB and multispectral imaging devices mounted on a UAV to identify weed infestation in winter wheat. Bascon et al. (2022) used UAV based multispectral imagery for rice yield prediction. Campos et al. (2020) used multispectral camera mounted on a UAV for variable rate application of pesticides in vineyards.

3.3. Hyperspectral imaging

Hyperspectral Imaging consists of continuous narrow bands with spectral resolution of 10 – 20 nm. Hyperspectral image can contain hundreds of bands of electromagnetic spectrum and has more informational content as compared to multispectral imaging but complexity is escalated due to the presence of redundant information. Hyperspectral imaging has high spatial and temporal resolution which makes it possible to distinguish smaller features and changes in plant health as well as soil degradation and changes in other environmental factors. While multispectral imaging can provide information about plant health in general with the help of vegetation reflectance in visible, near infrared and red edge region, hyperspectral information can be

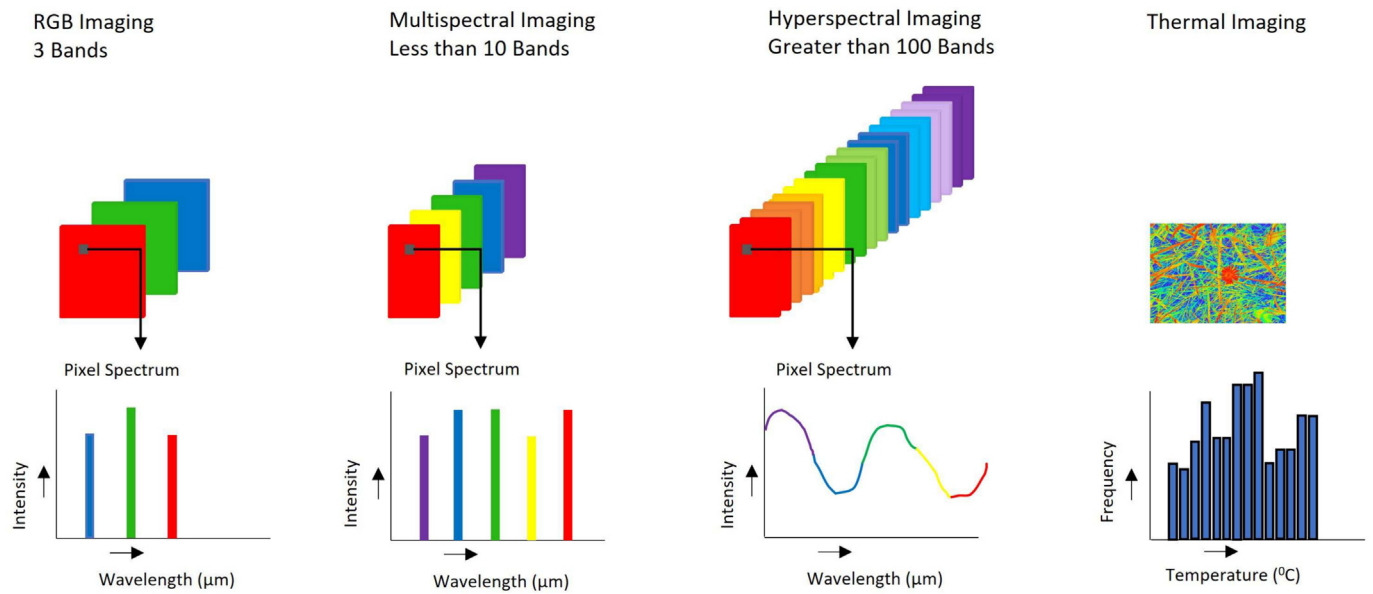


Fig. 3. Image acquisition techniques.

used to identify specific diseases, weeds or pests based on the unique spectral signature of each crop and vegetation including weeds. Hyperspectral imaging is mostly used for crop classification and weed identification. Photochemical reflectance index can also be used to measure water stresses. Datta et al. (2023) used hyperspectral imagery for soil properties characterization. Data obtained through the imaging device included 125 spectral channels of 4 nm spectral resolution in range 450–950 nm. Moghadam et al. (2017) used two different hyperspectral cameras for disease detection in capsicum plants. Short wavelength infrared (SWIR) hyperspectral camera with the spectral range of 900–2500 nm providing 168 spectral bands. Visible and near infrared (VNIR) camera with a spectral range of 400–1000 nm providing 324 spectral bands. Elvanidi et al. (2018) used a spectroradiometer with the spectral range of 350–2500 nm and a VNIR camera with the range 400–1000 nm to measure water and nitrogen stress in tomato crop.

3.4. Thermal imaging

Thermal imaging senses infrared radiation emitted by an object to produce a thermal image of the corresponding object. It can be used to detect water stresses in crops considering that the temperature for the plants under water stress is higher as compared to unstressed plants. Espinoza et al. (2017) used a combination of a multispectral camera and a thermal infrared camera for water stress identification in grapevine. They used a UAV to collect the images from both the sensors. Quebrajo et al. (2018) also used a thermal infrared camera mounted on a UAV for sugarbeet irrigation management. Thermal imaging can also be useful in the defect detection and identification of diseases and pests in crops. Batchuluun et al. (2022) collected a thermal plant dataset for disease detection in rice crop using deep learning approach. Kuzy et al. (2018) developed a pulsed thermographic imaging system utilizing a thermal infrared camera for blueberry bruise detection. Melesse et al. (2022) used a thermal camera for quality assessment of banana fruit during storage time.

Farmers are increasingly turning to latest imaging technologies, especially drones, for more precise monitoring solutions as compared to satellite images, resulting in better agricultural throughput, reduced risk and improved precision agriculture practices. Drones have revolutionized the industry by providing farmers with multi-spectral imaging information, allowing them to better assess crop health, which was not possible with traditional satellite imagery. By combining Global

Positioning System (GPS) technology with field maps, farmers can now make informed decisions regarding precision agriculture applications.

4. Image stitching and photogrammetry

Image stitching is used for the generation of a panoramic picture from two or more overlapping images. Main tasks in image stitching are image alignment and blending. During the image alignment process, correspondence among overlapping images is established. The two main approaches for alignment are direct and feature based techniques (Adel et al., 2014).

Direct techniques use a pixel-wise comparison to establish the overlap between various images of the same scene. Feature based techniques use key point matching to find the alignment between images. After identifying the overlap, appropriate transformations are applied to align the images for the registration process. Finally, blending is done to ensure seamless transition between images by removing harsh lines and ghosting artefacts caused during to image registration process. Image stitching workflow is given in Fig. 4.

Researchers have explored various methods for implementing image stitching. Abbadi et al. (2021); Mehrish et al. (2014); Megha and Rajkumar (2022) have provided detailed comparison of different approaches used in image stitching.

Many researchers have worked on the improvement of the existing image stitching techniques. Liu et al. (2022) proposed a fast scale-invariant feature transform (SIFT) algorithm for image stitching for the detection of straw return rate in the Blackland areas of China. They performed histogram equalization and noise removal as a preprocessing step on drone images before applying an optimized SIFT algorithm. Their algorithm performed down-sampling to reduce the number of key-points to be matched in images and then used MN SIFT descriptor that is based on normalized gradients to improve speed. To improve the accuracy of matched key-points, they used the progressive sample consistency (PROSAC) algorithm. For image fusion, they performed optimal stitching line detection along with fading in and fading out method. The sutures in the overlapping region were detected based on texture, color and gradient difference. For multiple image stitching, a layered approach was used in which images acquired from the same aerial route were stitched first to get layers containing multiple images stitched together. Then the panoramic result of each image layer was

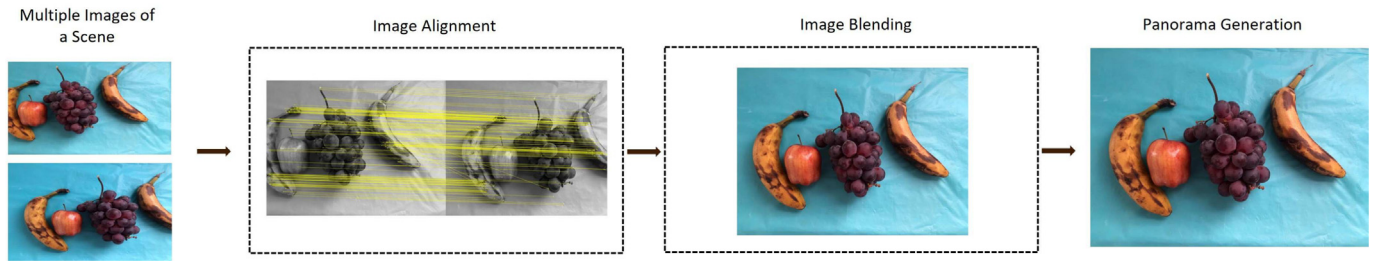


Fig. 4. Image stitching workflow.

stitched to get the final full panoramic image. Their algorithm has been reported to be more optimized and fast as compared to traditional SIFT and speeded up robust features (SURF) based methods. Lee et al. (2020) presented an improved stitching method based on optical flow algorithm. They claimed that a better 360° panorama can be generated using optical flow algorithm as compared to traditional feature-based techniques which lacked accuracy because of variation in the depth of projected area. After identifying the overlapping region through feature matching, correction in the seam of overlapping area was performed using the motion fields based on the values of pixels in the corresponding region. Their method worked best for the real-time stitching of images. Gao et al. (2023) proposed an improved fusion algorithm for removing the discontinuities in stitching process. They improved the feature matching using the binary robust invariant scalable keypoints (BRISK) and grid-based motion statistics (GMS) algorithm. Seam line was found using optimal seam algorithm and fusion was done using fade-in fade-out weighting algorithm. The research was aimed at providing an improvement in image stitching based on fast image algorithms. Tang et al. (2023) proposed an improvement of image warping method using an adaptive triangular mesh-based optimization technique. Their technique used feature points and uniform points as grid vertices. The proportion of each image part was found on the base of the distance between vertices and the nearest feature points. Their method successfully removed the ghosting effects and produced better looking panoramic images. Li et al. (2017) improved the stitching process by implementing an enhanced weighted fusion algorithm that eliminated the motion-based ghosting effect; however, their video fusion technique was relatively slow and needed improvement for real-time implementation. Yu et al. (2023) used SIFT for feature detection and Local Graph Structure Consensus (LGSC) for outlier removal. Then they used a local mesh alignment method for pre-warping images. Images were divided into grids and local homography for each mesh was generated for better alignment. Image fusion was done after energy function generation and linear blending where line segment detector (LSD) algorithm (Gioi et al., 2010) was used for line segment detection. Energy function was defined using point and line correspondences, and structure preservation such that linear structure would not appear bent during warping and the boundary of the resulting image remained rectangular. Their method provided better alignment results with structure preservation but time complexity became higher with increasing number of images and high resolution thus preventing real-time performance. Yuan et al. (2021) proposed a superpixel-based stitching technique. In the first step, their method performed adaptive as-natural-as-possible (AANAP) image registration method. Then simple linear iterative clustering (SLIC) algorithm was used to segment the overlapping region into super pixels. The energy function was proposed based on texture complexity, color difference and gradient difference information to find optimal seam line. At the end superpixel-based color blending was performed to obtain final results. A comparison of various stitching approaches is presented in Table 2.

Agricultural field mapping can be done using image stitching techniques that can generate a connected and continuous

panoramic image. Image stitching can work with fewer key points and small overlap between the images (a 30% overlap is normally sufficient for many applications). It works well with small datasets in flat terrain applications. For non-flat terrains, image artefacts are generated due to misalignment of objects in various photos. Furthermore, in non-flat terrains, the scale is not preserved and vary based on the distance of each point from the camera (Pix4D, 2021). Generation of more accurate and precise orthomosaics from aerial photos requires the use of photogrammetry. Photogrammetry is an image stitching technique that generates rectified panoramas such that distances are preserved and geometric distortion is removed. It provides better and precise results as compared to simple image stitching, however the process is computationally extensive and high overlapping between the images is needed. Normally an 80% overlap is required for generating an orthophoto from photogrammetry process. Digital Surface Models (DSMs) are used for removing perspective distortion and scale difference from connected images to generate orthomosaics that are orthorectified and are called true orthophotos. True orthophoto generation is an important step in agricultural drone mapping. Farmers can make use of high-resolution drone maps with fields' boundary and vegetation information for monitoring and surveying the farmlands and consequently making improved decisions for better crop production. They can compare the growth of crops at various times of year, identify diseases and pest infestations, make prescription maps for application of fertilizer, herbicides and pesticides, analyze the moisture content in plants and soil to modify irrigation system, and plan the harvest.

The quality of orthomosaics depends mainly on the overlap percentage. Mesas-Carrascosa et al. (2017) compared the effect of varying flight parameters on the accuracy of orthomosaics using the Agisoft Photoscan Software. Seven altitude/height values were chosen including 30, 40, 50, 60, 70, 80, and 90 m above the ground. Two overlap settings were selected including 60–30% and 70–40% endlap – sidelap values. Best photo quality was found with 60–90 m height of flight and 70–40% overlap. Ford et al. (2019) used Pix4D to generated orthophotos of thermal and multispectral images obtained of a corn and winter wheat fields. Usually orthomosaics are generated offline using various commercial tools or software. Zhao et al. (2020b) present an online method for photo stitching in mobile devices that works in low overlap cases. Table 3 shows a non-exhaustive list of widely used photogrammetry tools commercially available.

5. Image analysis

Image analysis is performed to extract useful information from the images. Humans are subjective in visually evaluating data in fields. Image analysis using computer vision and machine learning technologies offers several advantages over humans such as fast speed, reliability and improved accuracy. The analysis techniques depend on the application under consideration. Some common steps might include pre-processing, orthomosaicing, feature extraction, plant segmentation,

Table 2
Comparison of stitching techniques.

Image alignment	Image fusion	Advantages	Reference
Optimized SIFT and PROSAC	Optimal stitch line with fade in fade out method	Fast and robust stitching	(Liu et al., 2022)
Equiangular plus optical flow	Motion field maps plus padding and interpolation	Interpolation time is long, good for real time stitching	(Lee et al., 2020)
BRISK detector, Brute force & GMS for matching	Optimal seam plus optimized fade in fade out weighted average fusion algorithm	Better stitch quality with reduced ghosting	(Gao et al., 2023)
SIFT and RANSAC	Triangular mesh deformation & joint optimization using energy function and APAP warp	Reduced ghosting effect	(Tang et al., 2023)
SIFT and RANSAC	Improved weighted average fusion	Improved speed and reduced ghosting	(Li et al., 2017)
SIFT and LGSC	Local mesh alignment, total energy function minimization & linear blending	Better alignment & structure preservation but high time complexity for real time performance	(Yu et al., 2023)
AANAP & SLIC for super pixel segmentation	Super pixel based energy function & color blending	Better stitching results with time efficiency	(Yuan et al., 2021)

SIFT - Scale invariant feature transform; PROSAC - Progressive sample consistency algorithm; SURF - Speeded up robust features; BRISK - Binary robust invariant scalable keypoints; GMS - Grid-based motion statistics algorithm; RANSAC - Random sample consensus; APAP - As-projective-as-possible; LGSC - Local Graph Structure Consensus; AANAP - As-natural-as-possible; SLIC - simple linear iterative clustering algorithm.

object recognition, and classification. In precision agriculture, image analysis is used for estimating crop metrics, devising treatment plans, and decision-making. Some application areas utilizing image analysis techniques are explored in this section.

5.1. Soil monitoring

Soil health and property characterization are sometimes necessary for better agricultural productivity. One important property is soil texture that has an effect on many other soil properties such as infiltration, water holding, and potential of hydrogen (PH) buffering capacities. Soil organic matter (SOM) is another property that affects the quality of soil and influences other soil properties. Soil nitrogen defines the fertility of soil while soil moisture characterization is done to predict water requirements. Traditional laboratory testing methods for measuring soil characteristics are costly and time consuming. Vision-guided systems

can be used for soil data collection and analysis for measuring various important properties of soil that can be then utilized by farmers to make informed decisions on the amount of fertilizer needed and to plan irrigation schedules accordingly. Fig. 5 presents the workflow of a vision-guided soil monitoring system. Images of soil samples are obtained and analyzed using various image processing and computer vision techniques for the extraction of useful information. This information is then used by machine learning algorithms to make predictions about the soil properties. At the end, decision about the farming requirements are made with the help of estimated quantities.

In literature, various computer vision and machine learning techniques have been utilized for analyzing different soil properties. Sudarsan et al. (2016) presented a microscope-based imaging system for soil texture and organic matter characterization. They applied median filter during preprocessing to remove the noise caused by micro vibrations during soil sample handling. Image segmentation was done using adaptive Otsu thresholding. Number of objects was found using connected component labeling technique. Small holes were identified using blob analysis and filled using flood fill method. Watershed algorithm was applied for image segmentation. The features computed included the values of hue, saturation, and value parameters, porosity and local variance matrices with three window sizes on the masked as well as the original images. They used linear regression to define a predictive relationship between the calculated parameters through image analysis and laboratory-measured properties including sand, silt, clay and SOM composition. The R2 values for the testing dataset for SOM and sand content was 0.83 and 0.63, respectively. Yang et al. (2021b) used hyperspectral imaging to measure various soil characteristics including SOM and soil total nitrogen (STN). Competitive adaptive reweighted sampling (CARS) and successive projections algorithm (SPA) were used for selection of hyperspectral bands containing necessary information about the desired characteristics. For prediction, particle swarm optimization (PSO) was used with extreme learning machines (ELM) algorithm. Hyperspectral vegetation indices are numbers obtained from the reflectance bands to study the stress and biochemical properties of plants. Yang et al. (2021a) studied relationship between the carbon content of soil and hyperspectral indices. They constructed their model using partial least squares regression. They reported that the relationship between spectral characteristics and soil organic carbon (SOC) content could be improved using differential transformations. Another important application is the development of smart irrigation systems which supply exactly the right amount of water depending on the requirements of the land estimated using soil analysis. Al-Naji et al. (2021) used RGB camera and AI to perform color analysis of soil for predicting the water requirement. Soil images were taken under varying illumination and water conditions of soil (dry or wet). Change in color values of the soil could be because of the water content or

Table 3
A non-exhaustive list of commercially available photogrammetry tools.

Software	Pros	Cons
Pix4D	Windows, macOS, Android, iOS support Different versions for different industries	High Price (\$350/monthly subscription) Relatively slower
Drone Deploy	Easy teamwork owing to rich collaboration features available Windows, macOS, Android, iOS support	High Price (\$499/monthly subscription)
Agisoft Metashape	Real time orthomosaic generation Multiple types of drones are supported Efficient customer support services Windows, MacOS and Linux support	High Price for professional edition (\$3499 one time)
Correlator 3D	Extensive menu Fast performance for small datasets Generated models can be uploaded to web based platform support Fastest	Only supports Windows High Price (\$295/monthly)
WebODM	Good for agriculture applications Easy templates Supports Windows and macOS Free/opensource	Difficult installation Slow for large datasets
MicMac	Easy templates Windows and macOS support Free/opensource	More adapted to professional users

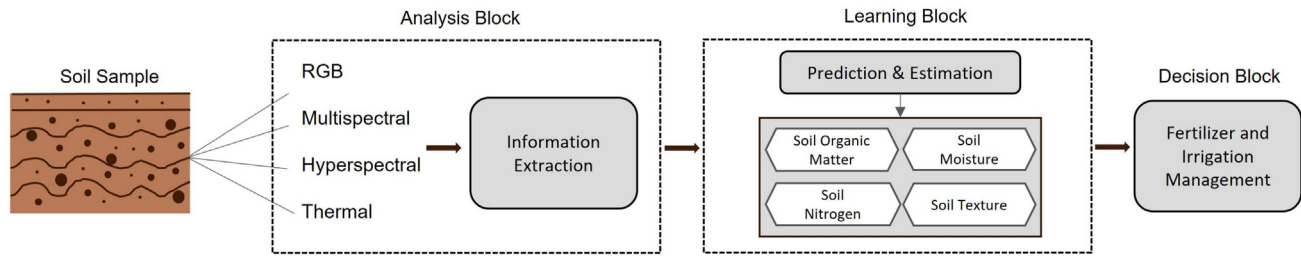


Fig. 5. Vision-guided soil monitoring and analysis.

varying illumination conditions due to sunny or cloudy weather. Feed forward backpropagation neural network was trained on the color channels for categorizing the soil condition. They reported MSE of 1.004×10^{-5} for test data. Liu (2022) proposed an imaging system for soil water content detection using color feature information. They performed a comparison of five different color spaces. Gaussian curve fitting on each channel was done to estimate the statistical parameters for the images. Least squares regression (LSR), Stepwise regression (STR), and partial least squares regression (PLSR) was performed at the end to predict the soil water content. Singh and Gaurav (2023) used Multispectral imagery from satellites to estimate surface soil moisture. For ground truth, universal random grid sampling method was used on field to measure soil moisture. Various preprocessing techniques were used for denoising and feature extraction. Various features from satellite data were extracted for final estimation including Latitude, Longitude, backscatter values, incidence angles, NDVI, digital elevation model (DEM) and two synthetic features from VV (vertical-vertical) and VH (vertical-horizontal) polarization data. Classification was performed using a feed forward neural network. Datta et al. (2023) estimated SOC, soil nitrogen and soil moisture based on hyperspectral data. Data cleaning was done to reduce inhomogeneity of the data, then standardization of data was done using data scaling. Empirical mode decomposition was performed to obtain intrinsic mode functions (IMFs) from the input data. PCA was used for dimensionality reduction. Performance of different predictive models including random forest, decision tree, gradient boosting, self organizing map, k nearest neighbors, artificial neural network, support vector regression and 1D convolution neural network (CNN) was compared.

They compared the results obtained using all hyperspectral bands, full range of visual bands and RGB values selected such that the mean reflectance of the blue band was in range 400–500 nm, green band in 500–600 nm, and red band in 600–700 nm. Best prediction results were obtained when a full range of visible spectrum was considered. Table 4 gives a comparison of various soil monitoring techniques.

5.2. Stress detection and targeted spraying

Plant stress indicates a condition that affects the normal growth of a plant. Crop yield and productivity are highly affected by stresses that can be caused by various environmental factors. Based on the causes, stresses can be divided into two categories: abiotic stresses and biotic stresses. Abiotic stresses are caused by the non-living components of an ecosystem. These may include very high or low temperature, insufficient or excessive water, salinity, radiations, or presence of heavy metal in the soil. Biotic stresses refer to the stresses caused by pests, fungi and other microorganisms that are a cause of various diseases in plants. Fig. 6 describes the workflow of an automated vision-guided system for detection of biotic and abiotic stresses in plants. The analysis block utilizes vision-based techniques to extract necessary information according to the application. This information is then forwarded to the learning block that classifies and predicts plant stresses. Decision block then makes necessary decisions about the irrigation requirements and targeted spraying of pesticides and fertilizers.

Water and nitrogen stresses are the abiotic stresses caused by excess or deficiency of water and nitrogen in plants. Nitrogen levels directly influence the final crop production. The estimation of nitrogen levels and

Table 4
Comparison of soil monitoring techniques.

Imaging Technique	Image Analysis Methods	Decision-Making / Prediction Techniques	Application	Reference
Digital microscope-based imaging	Thresholding; Connected component analysis; Watershed segmentation; Feature Extraction	Multivariate stepwise linear regression	Soil Texture & soil organic matter characterization	(Sudarsan et al., 2016)
Hyperspectral imaging	Multiplicative scattering correction for Denoising; Competitive adaptive reweighted sampling & successive projections algorithms for band selection	PSO & extreme learning machine algorithm	Soil organic matter & soil total nitrogen characterization	(Yang et al., 2021a)
Hyperspectral imaging	Simple, first order and second order differential transforms	Partial least square regression	Soil organic carbon content prediction	(Yang et al., 2021b)
RGB Imaging	Manual selection of ROI; Averaging of brightness values for ROI	Feed forward back propagation neural network	Soil irrigation requirement prediction	(Al-Naji et al., 2021)
RGB Imaging	ROI based on Thresholding; RGB to CIE & HLS color space transformations; Feature extraction	Least squares regression; Stepwise regression & partial least squares regression	Soil water content detection	(Liu, 2022)
Multispectral satellite imagery	Radiometric calibration; Multi-look correction; Speckle noise removal; terrain correction; Feature extraction	Feed forward artificial neural network	Surface soil moisture estimation	(Singh and Gaurav, 2023)
Hyperspectral data	Data cleaning and scaling; Visual band selection; Empirical mode decomposition; PCA	Random forest; Decision tree; Gradient boosting; Self organizing map; k-nearest neighbors; Artificial neural network; Support vector regression & 1D Convolution neural network	Soil Organic Carbon, Soil Nitrogen & Soil moisture characterization	(Datta et al., 2023)

RGB - Red-green-blue; PSO - Particle swarm optimization; ROI - Region of interest; PCA - Principle component analysis.

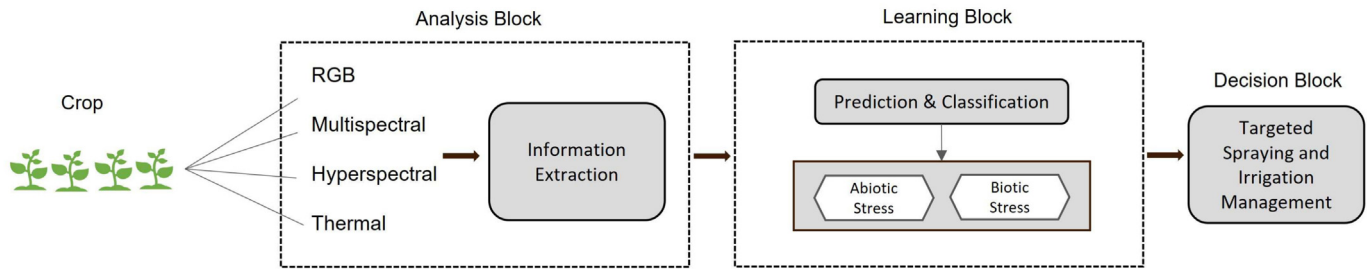


Fig. 6. Vision guided stress detection in crops.

the generation of prescription maps for precise fertilizer application at targeted locations are important applications of computer vision in agriculture. The necessary nitrogen level required for each crop varies depending upon the crop under consideration. Similarly, water stress in plants can be measured using automated techniques that enable the implementation of smart irrigation systems that use water as per requirement, thus optimizing the water consumption. Nitrogen deficiency is directly linked with the color and texture of leaves. Hence imaging techniques can be used for nitrogen level prediction. Various methods of nitrogen level detection have been implemented in literature. Haider et al. (2021) estimated nitrogen content in plant leaves based on color features extracted from RGB images of leaves and by comparing them with the reference color values. Zhao et al. (2021) have studied the relationship between plant growth indices and nitrogen content for winter wheat images by extracting the canopy cover. Adhikari

et al. (2020) estimated the nitrogen content using the reflectance ratio calculated from red and near infrared image channels. Colorado et al. (2020) (Colorado et al., 2020) use multispectral imagery and vegetation indices to measure nitrogen content in rice crop. Fu et al. (2021) give a detailed overview of the use of various hyperspectral techniques for nitrogen content estimation. Maresma et al. (2016) perform statistical analysis to define relationship between the amount of nitrogen applied and various vegetation indices and crop height. The vegetation indices were calculated from multispectral images. Elvanidi et al. (2018) found water and nitrogen deficit in tomato using hyperspectral imaging data. Classification tree was used to predict water and nitrogen contents using various reflectance indices. Mwinuka et al. (2022); Rubo and Zinkernagel (2022) focused on finding the relationship of nitrogen and water stress with different vegetation indices extracted using multispectral and hyperspectral imagery.

Table 5
Comparison of abiotic stress detection techniques.

Imaging Technique	Image Analysis Methods	Decision-Making/ Prediction Techniques	Application	Reference
RGB imaging	Thresholding; ROI detection using bounding box; ROI color detection	ROI color comparison with reference values	Nitrogen stress detection	(Haider et al., 2021)
RGB imaging	Canopy cover segmentation using thresholding on G-R channel values	Regression analysis using allometric curve	Relationship between plant growth indices & nitrogen status with plant canopy cover	(Zhao et al., 2021)
Multispectral imaging	Background segmentation using thresholding; Reflectance ratio from R & NIR mean values	Statistical analysis of Reflectance ratio & nitrogen content	Nitrogen content estimation	(Adhikari et al., 2020)
Multispectral Imaging	GrabCut & guided filter segmentation,	Multi-variable linear regression; support vector machines; Artificial neural networks	Nitrogen content estimation	(Colorado et al., 2020)
Multispectral Imaging	Image orthomosaicing; Vegetation indices calculation; Crop height estimation	Statistical analysis of vegetation indices, crop height and nitrogen	Nitrogen fertilizer requirement & crop yield prediction	(Maresma et al., 2016)
Hyperspectral imaging	Multiple reflectance indices calculation	Classification Regression tree for prediction	Water & nitrogen deficit stress detection	(Elvanidi et al., 2018)
Multispectral imaging	Image orthomosaicing; Multiple Vegetation indices calculation	Statistical analysis of vegetation indices	Water & nitrogen level management	(Mwinuka et al., 2022)
Hyperspectral imaging	Denosing and normalization; Multiple vegetation indices calculation	Statistical analysis of vegetation indices, CARS-PLSR and inflection points	Water, chlorophyll & nitrogen content estimation	(Rubo and Zinkernagel, 2022)
Thermal imaging	CWSI calculation based on canopy temperature values	Histogram analysis of crop water stress index & crown temperature	Water stress detection	(Agam et al., 2013)
Thermal & multispectral imaging	Normalized relative canopy temperature & spectral indices calculation	Statistical analysis	Water stress detection	(Elsayed et al., 2017)
Thermal & multispectral imaging	Average temperature, NDVI and GNDVI calculation	Statistical analysis	Water stress detection	(Espinoza et al., 2017)
Thermal imaging	Tree crown temperature & CWSI calculation	Statistical analysis	Water stress detection	(Gonzalez-dugo et al., 2013)
Thermal imaging	Mean temperature of vegetation cover & CWSI calculation	Statistical analysis	Water stress detection	(Quebrajo et al., 2018)
RGB imaging	Background segmentation; Binarization; Color segmentation; Feature extraction	SVM, KNN, Decision tree and CNN based classification	Nitrogen stress detection	(Azimi et al., 2021a)
RGB imaging	CNN based feature extraction	CNN-LSTM for classification	Water stress detection	(Azimi et al., 2021b)
RGB imaging	Image cropping	MobileNet, Mnasnet and EfficientNet for classification	Water stress detection	(Kamarudin and Ismail, 2022)

ROI - Region of interest; RGB - Red-green-blue; G-R - Green-Red; R - Red; NIR - Near infrared; CARS - Competitive adaptive reweighted sampling; PLSR - Partial least square regression; CWSI - Crop water stress index; NDVI - Normalized difference vegetation index; GNDVI - Green normalized difference vegetation index; SVM - Support vector machine; KNN - K nearest neighbor classifier; CNN - Convolutional neural network; LSTM - Long short term memory network.

Thermal imaging of plants is another way of measuring water stress since there is a direct relationship between water stress and temperature of leaves. Researchers including (Agam et al., 2013; Elsayed et al., 2017; Espinoza et al., 2017; Gonzalez-dugo et al., 2013; Quebrajo et al., 2018) have focused on the use of thermal imaging techniques to precisely map the water content of a land for enhancing water usage efficiency.

Apart from traditional spectral indices-based stress detection, some researches focus on using the deep learning techniques for nitrogen and water level detection in plants. Azimi et al. (2021a) proposed a 23 layered CNN architecture for nitrogen stress indication using RGB imaging. Their proposed network outperformed the traditional machine learning methods by attaining 8.25% better accuracy. Considering the shortcoming of traditional methods of stress detection, which normally require severe stress signs to be visible for reliable detection, Azimi et al. (2021b) applied temporal analysis on visual stress symptoms in chickpea plants using long short-term memory (LSTM) network. Their network achieved an accuracy of 98.5% on publicly available datasets of chickpea shoot images. Chandel et al. (2021) compare the performance of three neural network architectures including AlexNet, GoogleNet and InceptionV3 for water stress detection in maize, okra, and soybean crops. Their results showed that GoogleNet performed best by achieving an accuracy of 98.3%. Kamarudin and Ismail (2022) used visible and near infrared imagery and light weight CNN model for detecting water stressed plants. Their EfficientNet model was able to get an accuracy of more than 88%. A comparison of abiotic stress detection techniques is given in Table 5.

Biotic stress includes harm caused to crops by the biological components of the ecosystem. Early stress identification is crucial to prevent crop losses in later stages. An estimated 30–40% crop loss is suffered globally due to plant diseases caused solely by insects (García-Lara and Saldívar, 2016). Researchers have tried various visual analysis and classification techniques for biotic stress detection in plants. Qin et al. (2016) compare three traditional machine learning techniques including support vector machine (SVM), random forest classifier and k nearest neighbor classifier for classifying four alfalfa leaf diseases. Islam et al. (2017) implemented potato disease classification using an SVM classifier. Saleem et al. (2022) proposed a region-based fully convolutional network (RFCN) for disease detection in multiple crops including pear, apple, avocado, kiwifruit and grapevine. A 93.8% mean precision was reported for this model. Zhang et al. (2022) detected grape downy mildew disease using YOLOv5-CA technique by integrating a coordinate attention technique with YOLOv5 architecture. Mean accuracy of their system was reported as 89.55%. Esgario et al. (2020) used ResNet50 architecture for biotic stress detection in coffee leaves. They reported an accuracy of 95.24%. Fraccaro et al. (2022) used UNET-ResNet34 encoder-decoder configuration for classification of weed in winter wheat crop. A pixel-wise segmentation approach was used to classify each pixel of an image to weed or background. They reported an accuracy of 90%. Hu et al. (2021) present a semi-supervised deep learning approach for weed classification in images without the need for labeling the data. They trained the teacher model on synthetic images, and then Faster RCNN (Region-based convolutional neural networks) was used to generate pseudo labels for the unlabeled data. Afterwards, the student model was finetuned on the weights obtained through the teacher model on synthetic and pseudo-labeled data collectively. Their weed detection model had the performance comparable with supervised methods. Chang and Lin (2018) proposed a machine that could perform weeding and variable rate irrigation using image processing and segmentation techniques. They used color information to extract soil moisture content.

Overexposure to pesticides, herbicides and other chemicals causes significant crop losses worldwide. Site-specific spraying allows less use of chemicals hence increasing the environment sustainability. Furthermore, with the help of latest drone technology, it is possible to automate the spraying process. Computer vision techniques combined

with traditional or more recent deep learning models have been widely explored in literature for generating prescription maps for targeted spraying using unmanned air vehicle (UAV). Huang et al. (2018) performed pixel-level classification using fully convolutional networks (FCNs) on drone images of a rice field for weed detection. They first generated an orthomosaic image of the field from UAV imagery. Then classification was performed to find the weed cover map. This cover map was then segmented based on chessboard segmentation process to find the targeted spraying area based on percentage of weed cover in the grid. Khan et al. (2021) proposed a two-step process for real-time spraying area recognition for UAV-based spraying. They first extract color and shape information from UAV images and forward this information to a target recognition module which then performed classification in two phases. Training and testing were done in offline phase using CNN. In online step, the real time input was classified using the data from first step and trained classifier. They were able to get an F1 score of 0.965. Authors in (Li et al., 2022) designed a real-time weed spraying system using an RGB camera-based imaging system and deep learning classifiers. They designed a spraying system using microcontroller and solenoid valve. Their camera module captured the images and sent it to the onboard computing device that identified the target area to be sprayed based on a trained neural network in real-time. They used YOLOv5s architecture after replacing the backbone with MobileNetv3 to obtain a lightweight version of the classifier. Acharya (2023) proposed a method for spray area identification along with the necessary spray cone angle determination using CNN. Thorat et al. (2023) proposed a system based on transition probability function (TPF), and CNN to identify pests and recommend the insecticides needed for targeted spraying. Their image-dataset consisted of the images of pests. A 28-layered CNN was used for classification of five types of insect classes and based on the probability of each insect, corresponding insecticide was recommended. Farooque et al. (2023) proposed a smart variable rate multi purpose sprayer for agrochemical application in potato field. They used three cameras to take the images simultaneously from different rows in the farm for weed and disease detection. YOLOv3-tiny architecture was implemented for classification. Their system was able to reduce the herbicide and pesticide application by 47% and 51%. Campos et al. (2020) designed a variable rate sprayer. Multispectral images were used to obtain the vigor maps for grapevine. Pesticide application rate was determined using a decision support system, Dosavina, with the help of the canopy structural characteristics. Variable rate sprayer was successfully able to adjust the working parameters according to the prescription maps. A comparison of biotic stress detection and targeted spraying techniques is given in Table 6.

5.3. Crop yield estimation

Crop yield estimation is important for several reasons. National level crop estimates determine the market prices a consumer has to pay once the commodity is available in the market. Personal level crop estimates allow farmers to plan their budget accordingly. Crop yield is affected by many factors including diseases, pests, deficiency of nutrients, water, and soil characteristics. By having an accurate estimate of yield, farmers can have a better idea about the cumulative effect of contributing factors and thus can make informed decisions about the fertilization, agrochemical applications and harvest, etc. General workflow of crop yield estimation using machine vision is given in Fig. 7. Crop images are acquired using imaging techniques for data extraction in analysis step. The predictions are done using learning techniques for crop yield estimation using the analyzed data. Planning is done according to the predictions obtained by the system.

Different methods for yield estimation using vision-based techniques have been explored by the researchers in literature. Some of the latest techniques are summarized in Table 7. Kestur et al. (2019) presented an algorithm for counting mangoes focusing on yield estimation problem. MangoNet, their deep learning architecture for mangoes

Table 6
Comparison of biotic stress detection and targeted spraying techniques.

Imaging Technique	Image Analysis Methods	Decision-Making/ Prediction Techniques	Application	Reference
RGB imaging	Cropping; clustering & lesion segmentation; Color, shape and texture feature extraction	Random forest, SVM and KNN classifiers	Alfafa leaf disease detection	(Qin et al., 2016)
RGB imaging	Leaf segmentation; Color and texture feature extraction	SVM classifier	Potato leaf disease detection	(Islam et al., 2017)
RGB imaging	Data augmentation & annotation	Region-based fully convolutional network for classification	Disease detection in five horticulture crops	(Saleem et al., 2022)
RGB imaging	Manual data annotation	YOLOv5 with coordinate attention for classification	Grape leaf disease detection	(Zhang et al., 2022)
RGB imaging	Image cropping, Data augmentation	AlexNet; GoogLeNet; VGG16; MobileNetv2; ResNet50	Coffee leaf biotic stress detection	(Esgario et al., 2020)
RGB & multispectral imaging	Image tiling & Downsampling of background class	UNET-ResNet architecture	Weed detection in winter wheat crop	(Fraccaro et al., 2022)
RGB imaging	Image synthesis	Faster RCNN	Weed detection in cotton crop	(Hu et al., 2021)
RGB imaging	Adaptive thresholding; Morphological processing; Foreground segmentation; Wet distribution area of surface soil estimation using mean RGB values	Area based classification of plant & weed; Fuzzy logic controller for variable rate irrigation	Weed detection & Variable rate irrigation	(Chang and Lin, 2018)
RGB imaging	Orthomosaicing	Fully convolutional neural network for weed detection; Chessboard segmentation & Thresholding of weed cover map for prescription map	Site-specific weed management & prescription map generation	(Huang et al., 2018)
RGB imaging	Video to image conversion; Color and shape information extraction; Offline training and simulation	Convolutional Neural Network for classification	Weed detection & Targeted spraying	(Khan et al., 2021)
RGB imaging	Image annotation; Single layer grid & target prediction box generation for spraying module	Lightweight YOLOv5s for weed classification; Thresholding on the intersection area for targeted spraying	Weed detection & Targeted pesticide spraying	(Li et al., 2022)
RGB imaging	–	Transition probability function-Convolutional neural network	Targeted insecticide & Fertilizer application	(Thorat et al., 2023)
RGB imaging	Image annotation & labeling	YOLOv3 tiny	Targeted spraying of agrochemicals	(Farooque et al., 2023)
Multispectral imaging	Orthophoto maps; NDVI calculation; Vigor map generation based on thresholding	Decision Support System Dosavina	Variable rate application of pesticides	(Campos et al., 2020)

RGB - Red-green-blue; SVM - Support vector machine; KNN - K nearest neighbors; RCNN - Region-based convolutional neural networks; NDVI - Normalized difference vegetation index.

detection and counting was designed based on semantic segmentation. Images were taken from an RGB camera. They used more than 11,000 image patches with pixel-level class labeling, obtained from 40 images for training while 1500 image patches obtained from 4 images were used for testing purpose. Mangoes were detected from connected component detection on the output of MangoNet. The training was performed in two steps due to imbalanced classes. In the first step, network was trained on a subset of images with at least one mango. In second step, training was done on the entire dataset. Their F1 score was reported as 63.2%. Danilevicz et al. (2021) proposed an early yield prediction method based on multispectral imagery for maize crop. They used a multimodal approach by combining the genotype

information with multispectral data. The experimental field data including parental lines, source of seed, fertilizer, date of plantation, and number of days after sowing of seeds was used for prediction using tabular deep neural network. Another deep neural network was trained using multispectral images and the vegetation indices. The output weights of both the modules were then fed as input to the fusion module for prediction. They compared the performance of the predictions obtained through individual modules against the one obtained by the fusion module. It was found that the performance greatly improved after fusion with a root mean square error (RMSE) of 1.07 t/ha. Zhang et al. (2020) found the correlation between various spectral indices and the estimated yield of the winter wheat crop. Yield model was generated

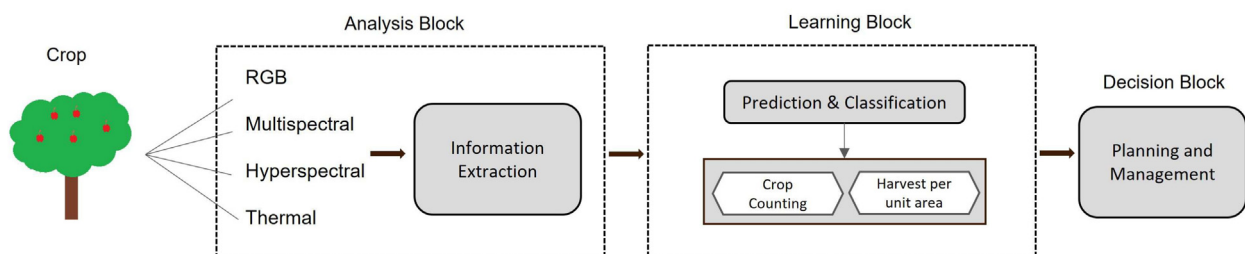


Fig. 7. Vision-based crop yield prediction.

Table 7
Comparison of yield estimation techniques.

Imaging Technique	Image Analysis Methods	Decision-Making/ Prediction Techniques	Application	Reference
RGB imaging	Data annotation; Semantic segmentation of images using deep convolution network	Connected object detection	Mango detection & Counting	(Kestur et al., 2019)
Multispectral imaging	Orthomosaic generation; Vegetation indices calculation	Random forest; XGBoost; Deep neural network	Maize crop yield estimation	(Danilevicz et al., 2021)
Multispectral Satellite imaging	Satellite image preprocessing; Vegetation indices calculation	Partial Least Square Regression	Winter wheat yield estimation	(Zhang et al., 2020)
RGB imaging	Data Annotation & Augmentation	SegNet	Tomato yield estimation	(Maheswari et al., 2022)
Multispectral Satellite imaging	Irregular data transformation based on thresholding; Image resizing	Combined 3D convolutional and recurrent neural networks	Crop yield estimation	(Qiao et al., 2021)
Multispectral imaging	Orthomosaicing; Mean reflectance values & vegetation indices calculation	XGboost algorithm	Rice grain yield prediction	(Bascon et al., 2022)
RGB imaging	Data augmentation; Spatial filtering & Contrast enhancement; Ensembled classification	Random forest, gradient boosting, linear regression & tree regression for yield prediction	Crop type classification & yield estimation	(Ilyas et al., 2023)

RGB - Red-green-blue; XGboost - Extreme gradient boosting algorithm.

based on partial least square (PLS) algorithm using four vegetation indices including GNDVI, optimized soil-adjusted vegetation index (OSAVI), NDVI and PSRI. The RMSE for predicted and measured yield were 693.9 kg/ha and 786.5kg/ha. Maheswari et al. (2022) proposed a tomato yield estimation system using deep learning-based semantic segmentation. RGB images of tomatoes were obtained from greenhouse environment. The ground truth annotation was done for background, ripe, and unripe tomatoes. Data augmentation using translation and rotation was performed. For classification they used SegNet architecture with 16 layers of VGG19 for feature extraction. They replaced the maxpooling layer by upsampling. They reported an F1 score of 80.22%. Qiao et al. (2021) proposed a module for extracting spatial and spectral features based on 3D CNN to capture the correlation between bands along with the spatial and spectral information. They also proposed a bidirectional recurrent neural network for capturing the temporal information from multi-spectral and multi-temporal images. In order to cope with the challenge of irregular shaped fields, they use data transformation based on thresholding and image resizing as preprocessing steps before inputting the data into deep network models. They reported an average RMSE of 0.84. Bascon et al. (2022) predicted rice yield using estimated aboveground biomass (AGB) and leaf area index (LAI) from the vegetation indices calculated from multispectral imagery. Ilyas et al. (2023) proposed an ensembled classification method for crop type classification and yield estimation. They used spatial filtering, scaling, flipping, shearing, and zooming to enhance the images. Then they performed ensembled classification using Adaboost, Decision Tree, Naive Bayes, Random Forest and Logistic Regression for crop type classification. For yield prediction they compared the performance of random forest, gradient boosting, linear regression, and tree regressor out of which the best prediction was resulted by gradient boosting algorithm. van Klompenburg et al. (2020) have provided details of studies implementing deep learning for crop yield estimation.

5.4. Quality control

Automated quality inspection and grading of agricultural produce is important for many aspects including food sustainability and reduction in food loss. Early defect detection is crucial for better shelf life of the produce. Considering that high quality products can generate more revenue, supply chain experts can use vision-based quality assessment to assign the items based on their predefined quality parameters to various sale channels depending on customer preferences. Vision-guided intelligent systems are more consistent and objective as compared to the manual counterparts making quality assessment more reliable. As shown in Fig. 8, produce images are analyzed using machine vision and image processing, and the extracted data is used to predict the quality for grading and sorting accordingly.

Researchers throughout the years have explored various techniques for defect detection and quality grading of fruits and vegetables. Summary of some latest techniques is given in Table 8. Santos Pereira et al. (2018) predicted the ripeness of papaya fruit using random forest classifier and peel color factor. Classification was done for three maturity stages. The ground truth was obtained using pulp firmness scores of the fruit. Images of fruits were taken using an RGB camera. ROI was extracted using the saturation channel of hue-saturation-value (HSV) color space with thresholding technique. They extracted twenty-one color features based on RGB, HSV and Lab color spaces. Random forest classifier was used to predict the ripeness based on extracted color features. They reported an accuracy of 94.3%. Abbas et al. (2019) proposed an apple grading and sorting system based on color, edge, and texture features extracted from fruit images taken using RGB camera. Conversion to HSV color space was done. Then binarization of V channel was done such that the defected part appeared white and remaining appeared black. Rotten parts were extracted using connected component analysis. A logical 'and' operation was used to combine the three types of feature images and depending on the area of white pixels in the

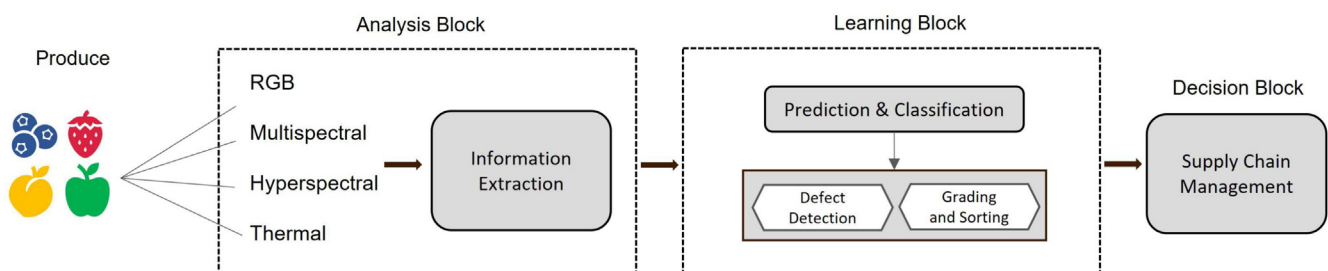


Fig. 8. Vision-guided quality control.

Table 8
Comparison of quality control techniques.

Imaging Technique	Image Analysis Methods	Decision-Making/ Prediction Techniques	Application	Reference
RGB imaging	ROI detection using thresholding; Color feature extraction	Random forest classifier	Ripeness level estimation of papaya fruit & Counting	(Santos Pereira et al., 2018)
RGB imaging	Noise removal; Binarization; Edge,color and texture feature extraction	Connected component analysis; Logical and operation & Area of rotten part	Apple grading and sorting	(Abbas et al., 2019)
Thermal imaging	Banana digital twin generation	Convolutional neural network	Quality assessment of banana	(Melesse et al., 2022)
RGB imaging	Noise removal; Histogram based apple segmentation; Morphological processing	Lightweight convolutional neural network	Apple defect detection	(Lee et al., 2023)
Thermal imaging	Edge detection; Background segmentation; Thresholding; Feature extraction	Linear discriminant analysis; Support vector machine; Random forest; K-nearest-neighbors & Logistic regression classifiers	Blueberry defect detection	(Kuzu et al., 2018)
Multispectral imaging	Color analysis for brown and healthy part detection (using smart color inspector); Browning ratio using logarithmic analysis	PLS for regression; ANN for classification	Internal mango browning detection	(Gabriels et al., 2020)
RGB imaging	Video to image conversion; Data labeling; MobileNetv2 for feature extraction	Path-Aggregation Feature Pyramid Network	Citrus sorting	(Chen et al., 2021)

RGB - Red-green-blue; ROI - Region of interest; PLS - Partial least square; ANN - Artificial neural network.

final image, defected fruit was identified. For good apple, resultant area would be zero. Melesse et al. (2022) proposed a new approach for quality assessment of banana fruit using digital twin method. The virtual replica was created based on thermal imaging data. The digital twin exactly replicated the original fruit regarding shape, size, and properties while reflecting the storage related changes occurring in the actual fruit. Thermal camera was connected to Internet of things (IoT) cloud services that utilized SAP Edge services for storage and monitoring of digital replica of the fruit. Thermal camera was used to take images at different stages of storage. The classification into four classes including rotten, fresh, good and bad was done using deep learning. Training was done in SAP intelligent service using feed forward convolutional neural network. They achieved an accuracy of 99%. Lee et al. (2023) proposed an apple defect detection system based on multicamera input. They used three cameras and rotation mechanism to completely and uniformly capture the complete surface area of an apple. They proposed an apple segmentation algorithm that utilized pyramid downsampling method to resize the image while keeping the shape, and then based on RGB color features performed apple segmentation. For resizing, minimum enclosing bounding rectangle was found and the image was cropped to only retain the apple area. CNN-based classification resulted in an accuracy of 93.8%. Kuzu et al. (2018) proposed a blueberry defect detection method based on thermal imaging. Images from two different cultivars of blueberries were obtained for classification. Destructive evaluation of bruised area was done and the images were analyzed to obtain the bruised area index which corresponded to the percentage of pixels in bruised tissue. Number of pixels in bruised area was found using edge detection and thresholding on green channel of destructive evaluation images. This feature was extracted for comparison with the classification results. Thresholding was performed on frames of berry videos to extract berry pixels. Time domain and frequency domain features were extracted. Five classifiers including linear discriminant analysis, SVM, random forest, logistic regression, and K-nearest-neighbors were selected and their performance was compared. Best classification accuracy was obtained from logistic regression classifier. Gabriels et al. (2020) determined healthy versus non-healthy mangoes based on internal browning in mango halves using visible and near infrared spectra. Browning index was calculated from mango halves images using smart color inspector (WUR, 2017). Ratio of color pixels of healthy and brown parts were determined. The natural logarithm of the ratio was taken to calculate internal browning in the mango. Classification was done by taking threshold on the calculated ratio and assigning class label 0 to mango with internal browning, and 1 to healthy mango using artificial neural network. PLS-based regression modeling was performed to find relation between spectra and the browning of mango. 83% test accuracy

on classification was reported. Chen et al. (2021) designed a system for sorting of oranges into three classes including healthy, mechanical damaged, and with skin lesions. A commercially available citrus processing line was used including a conveyor belt, webcam and led light for video recording. Defective fruit was detected using path-aggregation feature pyramid network (PANet). An algorithm for tracking the fruit on the conveyor belt using the SORT algorithm was also proposed. The detector and tracker combined accuracy was reported as 93.6%.

Nturambirwe and Opara (2020) have presented a detailed review of various techniques used for defect detection in horticulture products. Bhargava and Bansal (2021) present an analysis on various computer vision-based techniques used for fruit and vegetable quality inspection.

6. Decision making, treatment, and planning

For effective farm management and planning, the first step is to gather relevant data throughout the crop growth period, from soil preparation and seeding, to yield estimation and harvest. Spatial variability is an important factor that refers to variation of different parameters/conditions within an arable land. These parameters include variation in water and nutrient requirements, extent of disease and pest infestations, and other climatic factors that affect the growth of plants. Crop data collected throughout the growth period using multiple sensors helps in determining the spatial variability, that is useful in making informed decision about the next crop cycle. This data can be divided into four categories: (a) soil data including soil fertility and properties; (b) irrigation data including water requirements; (c) climate data such as humidity, wind and canopy temperature; (d) crop data including health and nutrient information at various growth stages, and quality and quantity of harvest. After data collection throughout the crop growth period, next step is the analysis and evaluation of this data to find the significance of each parameter and it's relevance to final output. Image analysis deals with the extraction of useful information from images acquired using various sources. Computer vision and image processing techniques convert raw data to a form that is better utilizable by traditional machine learning and more advanced deep learning techniques for making necessary predictions and estimations according to the application at hand as described in detail in Sections 5.1–5.4. These predictions and estimations are then conveyed to the farmer, who makes informed decisions about usage of resources, planning and management. The farmer is able to select a course of actions that is most profitable. From resource management and crop treatments to harvesting

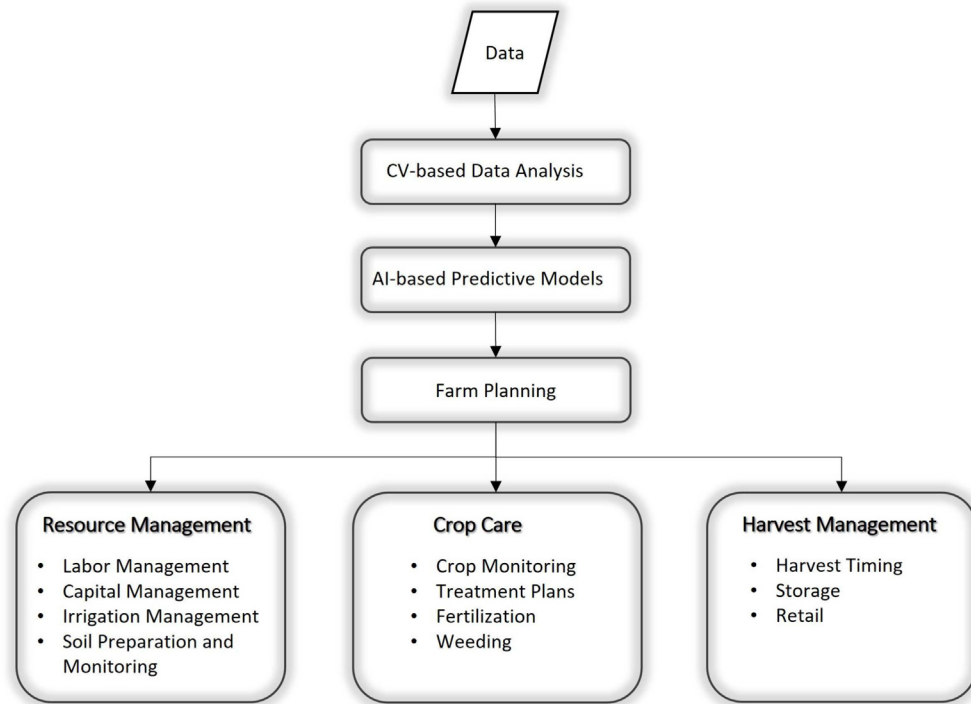


Fig. 9. Decision-making, treatment and planning.

and retail, effective management is possible. A block diagram, presenting various aspects of decision-making, treatments, and farm planning using imaging data, is shown in Fig. 9.

6.1. Resource management

One of the advantages of smart farming is better resource management. Land resources include soil type, fertility, drainage, and irrigation. Vision-guided soil monitoring data analysis and predictions can provide recommendations on the informed usage of fertilizers. Soil moisture level and water pattern estimations can help save water by planning irrigation schedules according to the water requirement. Right amount of nutrients and water can ensure healthy crops and high yield. Labor and capital resources management is also possible with the advancement in smart farming techniques.

6.2. Crop care

Crop monitoring is required at various growth stages to completely encompass spatial variability information. Using this information, farmer can make treatment plans accordingly for: (a) site-specific application of pesticides and herbicides; (b) fertilizer distribution; (c) weeding. With the predictions on the most likely time of pest infestation, farmers can not only take preventive measures to reduce the chances of crop being affected, but can generate maps of identified areas for targeted spraying that reduces the unnecessary application of agrochemicals consequently minimizing the cost and increasing yield.

6.3. Harvest management

Based on the spatial variability in quality and quantity of yield obtained through yield estimation maps, farmers can make informed decisions about the optimal timing of harvest. Farmers can plan accordingly to minimize potential crop damage caused by extreme weather events by planning to harvest earlier. Based on data analysis and predictions,

farmer can plan more effectively regarding post-harvest decisions including storage and retail.

7. Robotics in agriculture

The field of agriculture is undergoing a transition from traditional mechanization to the revolutionary automation with the long term goal of complete automation of agricultural farms. Traditional heavy farm machinery can cause soil compactness which is a cause of poor root growth consequently affecting the overall growth of plants. Advancement in the field of robotics and autonomous systems has shaped the future of multiple industries including the agricultural sector where traditional heavy farm equipment is now being replaced with advanced robotic systems that are intelligent, lightweight, and efficient. To fully automate the farming processes, robots need to work as a farmer and be able to 'see' and 'understand' the scene. State-of-the-art imaging sensors enable the robot to see and latest computer vision and AI techniques allow it to understand the environment. Fig. 10 provides an overview of robotics in smart agriculture and precision farming.

A fully automated farm may follow an integrated approach that combines various types of robots and autonomous systems working together in coordination. Ground vehicles can carry heavy loads and work for longer duration as compared to aerial vehicles which have limitations on loading and flight time. But aerial vehicles have a birds eye-view and are good for field mapping and monitoring. By adopting a cooperative approach, we can optimize the utilization of both vehicle types, effectively overcoming their individual shortcomings and unlocking their full potential for flawless operations. Although multi-robot systems are being investigated for efficient utilization in agricultural domain (Zhang and Noguchi, 2017; Pretto et al., 2021; Lal et al., 2017; Roldán et al., 2016; Janani et al., 2016), the research is still in its early stages, and significant advancements are required before complex tasks can be executed in real-world working conditions.

Before fully automated farms become a reality, a collaborative approach may be implemented in which robots work in collaboration with humans for delicate tasks, such as harvesting of soft fruits, pruning,

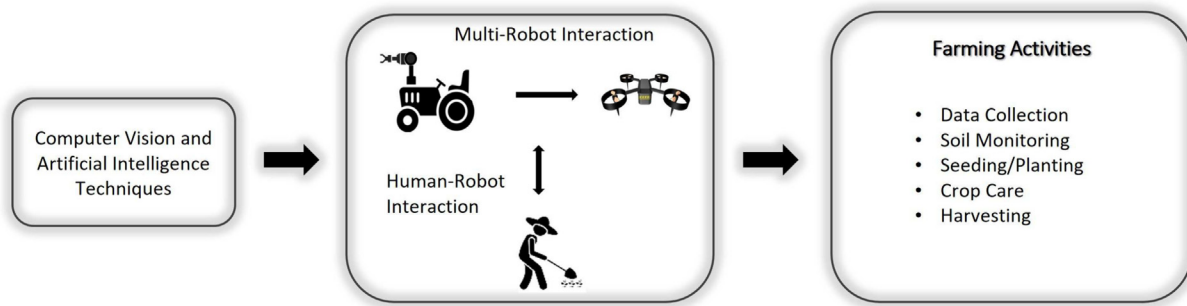


Fig. 10. Robotics in agriculture.

and spraying (Berenstein and Edan, 2012; Seyyedhasani et al., 2020; Guevara et al., 2021). Human-robot interaction (HRI) is an emerging area of research focused on exploring the strategic, social and ethical aspects of collaborative work environments, where robots and humans work together. Vázquez Hurtado et al. (2019) describe various approaches and challenges for HRI in agriculture. Effective communication, collaborative problem recognition and action implementation, and cooperative mission planning are key challenges in HRI. Robots not only need to be well aware of human presence, but they also need to predict the behavioral patterns for ensuring a safe and collision-free work environment.

Robotics technology has significantly strengthened the farming process in various ways, some of which are:

1. **Data Collection:** Robots equipped with latest imaging technologies and sensory devices are used in data collection for applications, such as soil monitoring, crop health inspection and growth pattern estimation. This data is important in understanding the spatial variability of crops, as described in Section 6. It can be used to create detailed field maps, identify areas requiring specific treatments, track livestock behavior patterns and optimize resource allocation.
2. **Crop Care:** Robotic systems employing cameras and machine vision technologies can be used for early detection of pest infestations and nutrient deficiency in crop that enables targeted application of agrochemicals on specified areas or individual plants consequently achieving high crop production and reduced chemical usage for environment sustainability.
3. **Automated Farming Tasks:** Robotic systems can be used for automation of various farming operations like seeding, weeding, planting, and harvesting. These automated systems are more efficient as compared to human workers and can work round the clock without intervention and provide a repeatable and reliable solution to the otherwise tedious farming operations. These automated systems improve the quality of tasks due to high precision, reducing the labor cost and increased productivity.
4. **Decision-Making:** Robotics technology is used to generate vast amount of data that makes data-driven decision making possible. With the help of state-of-the-art machine learning techniques, artificial intelligence algorithms and machine vision technology, farmers can gain invaluable insights into predicting and estimating various aspects of farming processes. This enables them to make informed decisions and optimize farming operations consequently enhancing the farm productivity.

Robotics technology has transformed the agriculture sector to become more sustainable and efficacious. The implementation of robotics technology in agriculture allows many advantages including reduced cost, improved productivity, enhanced farm management and overcoming the labor shortages.

8. Advances and challenges in fully automated smart farming

Each farming operation in fully automated smart farms involves a series of complex tasks that require precise coordination and decision-making, which can be challenging to automate. One step towards the realization of smart farms is the recent advancement in IoT-based sensing technology (Ullo and Sinha, 2021; Grgić et al., 2020; Friha et al., 2021). IoT with reference to agriculture refers to the network of interconnected devices, sensors, and equipment, including robots, deployed in farming operations to collect, transmit, and analyze data. In smart farms, mobile devices often rely on Internet connectivity for communication, especially when accessing cloud-based services. However, in areas with low connectivity, the IoT devices can communicate using wireless technologies like LoRaWAN (Bonilla et al., 2023) or Zigbee (Ramya et al., 2011) and then connect to the Internet through a gateway device, using a more reliable connection such as satellite or cellular networks. This enables data collection and transmission even in areas with limited Internet access, enhancing the effectiveness of smart farm technologies. Satellite IoT (Liu et al., 2023) is particularly valuable in agriculture, allowing for monitoring of large, remote farms and providing wide-area coverage for farm-monitoring applications.

Smart farms leverage mobile edge devices including UAVs, robotic harvesters, autonomous tractors, and other machinery, to automate tasks. However, deploying computer vision models on these edge devices pose challenges (Munir et al. (2021)). One issue is the need to limit model complexity and size due to constraints in computational power, memory, and battery life. Real-time processing is also challenging due to these resource constraints. Moreover, environmental factors in which these edge devices operate (e.g., lighting conditions, weather, and terrain) can affect the reliability and performance of these devices. To integrate smart edge devices with existing systems, a collaborative approach and specialized knowledge are required. To facilitate seamless integration and data exchange between IoT systems, lightweight protocols such as MQTT (Masdani and Darlis, 2018), which is designed for low-bandwidth, high-latency, or unreliable networks, and CoAP (Tariq et al., 2020), which is designed for constrained devices and networks, can be used. To overcome challenges like limited resources, lightweight and efficient computer vision models tailored for edge devices are crucial. Techniques like model compression, quantization, and efficient neural network architectures reduce complexity and resource requirements without sacrificing performance (Munir et al., 2024; Li et al., 2023; Tang et al., 2021; Hassan and Maji, 2022). Moreover, it is imperative to develop computer vision models that can adapt to challenges posed by harsh agricultural environments. Data augmentation techniques, such as adding noise or altering lighting conditions to the augmented data, can further enhance the robustness of these models. Development of low-cost hardware platforms and open-source software frameworks are necessary to enhance the affordability of smart agriculture solutions. Additionally, addressing resistance to change

and/or modernizing farming practices among traditional farmers is vital. Convincing these farmers to adopt disruptive technologies would require a combination of education and tangible evidence of the benefits these technologies can bring to farming. Furthermore, ensuring data security and privacy in smart agriculture is essential. Techniques such as data encryption, secure communication protocols, access control mechanisms, and robustness against adversarial attacks must be implemented to protect against unauthorized access and cyber-attacks, and to enhance the trustworthiness of digital data and the AI models.

To overcome these challenges, researchers must engage in innovative research for designing computer vision models tailored for agriculture and edge deployment considering the specific requirements and constraints of the challenging agricultural environment. Furthermore, outreach to farmers is very important to showcase the benefits of modernization and incorporation of digital and precision agriculture in farming practices. Overall, integrating IoT, mobile edge devices, and computer vision in smart agriculture has the potential to revolutionize the farming industry, and enhancing its efficiency, sustainability, and resilience.

9. Conclusions

This survey provides an extensive exploration of the digital life cycle of crops in precision agriculture, with a particular emphasis on the utilization of computer vision technology. The primary focus of this study revolves around reviewing the diverse techniques found in the literature which contribute to the development of vision-guided intelligent automated systems for precision farming.

This paper first discusses various pertinent crop metrics used in digital agriculture. Then this paper elaborates the usage of imaging and computer vision techniques in various phases of digital life cycle of crops in precision agriculture. The survey initially discusses various imaging technologies currently employed by researchers for acquiring essential imaging data in digital agriculture. Subsequently, it gives a brief overview of image stitching and photogrammetry for agricultural field mapping. A critical aspect of this study is a detailed discussion of image analysis and computer vision techniques applied to important precision farming tasks, with a particular focus on analysis and detection techniques for soil monitoring, stress detection, targeted spraying, yield estimation, and quality control. Furthermore, this paper provides a discussion on the implementation and utilization of analysis results for crop-planning and decision-making. Moreover, this survey provides a comprehensive discussion on the application of computer vision-assisted robotics in precision farming. Finally, the survey concludes by outlining the challenges in fully automated smart farming.

While image analysis techniques have been well-established in various industries, their successful implementation in vision-based analytic systems for precision agriculture tasks presents several challenges that need to be addressed. The performance of visual systems is largely affected by environmental factors like lighting conditions, weather changes, and occlusions caused by vegetation. Moreover, a vast amount of training data is required for effective execution of computer vision models. Additionally, obtaining accurate ground truth labels for big agricultural fields can be subjective and challenging. Another key challenge in making robust vision-guided intelligent systems for agriculture is lack of generalization of computer vision models that can work across multiple crop types. Models trained on one crop may not perform well on others, requiring extensive domain adaptation techniques. For fully autonomous farms, real-time detection, monitoring, and/or prediction of crop parameters are crucial; however, processing large amounts of image data in real-time can be computationally intensive and may require specialized hardware.

Addressing these challenges requires a combination of advanced computer vision techniques, data collection strategies, and domain expertise in agriculture. Collaboration between computer scientists,

agronomists, and agricultural experts is essential to develop robust, accurate, and practical stress detection systems that can contribute to more efficient and sustainable crop management practices. Based on the discussions in this paper, it can be concluded that, while the last decade has witnessed remarkable advancements in vision-guided intelligent systems, their implementation in the agricultural domain is still at an embryonic stage. The formidable challenges posed by harsh field conditions, unpredictable climatic factors, and various influences on crop conditions emphasize the need for extensive research and thorough field testing. Only through persistent exploration and engagement with farmers, the vision of fully automated agricultural farms can become a reality.

Declaration of competing interest

The authors declare that they have no known competing financial interests or personal relationships that could have appeared to influence the work reported in this paper.

Acknowledgements

This work was supported in part by the United States Department of Agriculture (USDA) National Institute of Food and Agriculture (NIFA), Award Number 2023-67021-40614. Any opinions, findings, and conclusions or recommendations expressed in this material are those of the author(s) and do not necessarily reflect the views of the USDA NIFA.

References

- Abbadi, N.K.E., Hassani, S.A.A., Abdulkhaleq, A.H., 2021. A review over panoramic image stitching techniques. *J. Phys. Conf. Ser.* 1999, 012115. <https://doi.org/10.1088/1742-6596/1999/1/012115>.
- Abbas, H.M.T., Abbas, T., Shakoor, U., Khan, J., Ahmed, M., Khurshid, K., 2019. Automated sorting and grading of agricultural products based on image processing. <https://doi.org/10.1109/ICICT47744.2019.9001971>.
- Acharya, P., 2023. A deep-learning framework for spray pattern segmentation and estimation in agricultural spraying systems. *Sci. Rep.* 13, 7545. <https://doi.org/10.1038/s41598-023-34320-7>.
- Adel, E., Elmog, M., El-Bakry, H., 2014. Image stitching based on feature extraction techniques: a survey. *Int. J. Comput. Appl.* 99, 1–8. <https://doi.org/10.5120/17374-7818>.
- Adhikari, R., Li, C., Kalbaugh, K., Nemali, K., 2020. A low-cost smartphone controlled sensor based on image analysis for estimating whole-plant tissue nitrogen (n) content in floriculture crops. *Comput. Electron. Agric.* 169, 105173. <https://doi.org/10.1016/j.compag.2019.105173>.
- Agam, N., Segal, E., Peeters, A., Levi, A., Dag, A., Yermiyahu, U., Ben-Gal, A., 2013. Spatial distribution of water status in irrigated olive orchards by thermal imaging. *Precis. Agric.* <https://doi.org/10.1007/s11119-013-9331-8>.
- Al-Najji, A., Fakhri, A.B., Gharghan, S.K., Chahl, J., 2021. Soil color analysis based on a rgb camera and an artificial neural network towards smart irrigation: a pilot study. *Heliyon* 7, e06078. <https://doi.org/10.1016/j.heliyon.2021.e06078>.
- Azimi, S., Kaur, T., Gandhi, T.K., 2021a. A deep learning approach to measure stress level in plants due to nitrogen deficiency. *Measurement* 173, 108650. <https://doi.org/10.1016/j.measurement.2020.108650>.
- Azimi, S., Wadhawan, R., Gandhi, T.K., 2021b. Intelligent monitoring of stress induced by water deficiency in plants using deep learning. *IEEE Trans. Instrum. Meas.* 70, 1–13. <https://doi.org/10.1109/TIM.2021.3111994>.
- Barnes, E., Clarke, T., Richards, S., Colaizzi, P., Haberland, J., Kostrzewski, M., Waller, P., Choi, C., Riley, E., Thompson, T., 2000. *Coincident Detection of Crop Water Stress, Nitrogen Status, and Canopy Density Using Ground Based Multispectral Data*.
- Bascon, M.V., Nakata, T., Shibata, S., Takata, I., Kobayashi, N., Kato, Y., Inoue, S., Doi, K., Murase, J., Nishiuchi, S., 2022. Estimating yield-related traits using uav-derived multispectral images to improve rice grain yield prediction. *Agriculture* 12. <https://doi.org/10.3390/agriculture12081141>.
- Batchuluun, G., Nam, S.H., Park, K.R., 2022. Deep learning-based plant classification and crop disease classification by thermal camera. *J. King Saud Univ. Comp. Inform. Sci.* 34, 10474–10486. <https://doi.org/10.1016/j.jksuci.2022.11.003>.
- Berenstein, R., Edan, Y., 2012. Human-robot cooperative precision spraying: collaboration levels and optimization function. *IFAC Proc.* 45, 799–804. <https://doi.org/10.3182/20120905-3-HR-2030.00084> 10th IFAC Symposium on Robot Control.
- Bhargava, A., Bansal, A., 2021. Fruits and vegetables quality evaluation using computer vision: a review. *J. King Saud Univ. Comp. Inform. Sci.* 33, 243–257. <https://doi.org/10.1016/j.jksuci.2018.06.002>.
- Bonilla, V., Campoverde, B., Yoo, S.G., 2023. A systematic literature review of lorawan: sensors and applications. *Sensors* 23, 8440. <https://doi.org/10.3390/s23208440>.
- Cai Gao, B., 1996. NDWI—a normalized difference water index for remote sensing of vegetation liquid water from space. *Remote Sens. Environ.* 58, 257–266. [https://doi.org/10.1016/S0034-4257\(96\)00067-3](https://doi.org/10.1016/S0034-4257(96)00067-3).

- Campbell, D.G.S., d. The researcher's complete guide to leaf area index (lai). <https://www.metergroup.com/en/meter-environment/education-guides/researchers-complete-guide-leaf-area-index-lai>.
- Campos, J., Gallart, M., Llop, J., Ortega, P., Salcedo, R., Gil, E., 2020. On-farm evaluation of prescription map-based variable rate application of pesticides in vineyards. *Agronomy* 10. <https://doi.org/10.3390/agronomy10010102>.
- Cao, X., Luo, Y., Zhou, Y., Fan, J., Xu, X., West, J.E.A., 2015. Detection of powdery mildew in two winter wheat plant densities and prediction of grain yield using canopy hyperspectral reflectance. *PLoS One* 10, e0121462. <https://doi.org/10.1371/journal.pone.0121462>.
- Chandel, N.S., Chakraborty, S.K., Rajwade, Y.A., Dubey, K., Tiwari, M.K., Jat, D., 2021. Identifying crop water stress using deep learning models. *Neural Comput. & Applic.* 33, 5353–5367. <https://doi.org/10.1007/s00521-020-05325-4>.
- Chang, C., Lin, K., 2018. Smart agricultural machine with a computer vision-based weeding and variable-rate irrigation scheme. *Robotics* 7. <https://doi.org/10.3390/robotics7030038>.
- Chen, Y., An, X., Gao, S., Li, S., Kang, H., 2021. A deep learning-based vision system combining detection and tracking for fast on-line citrus sorting. *Front. Plant Sci.* 12. <https://doi.org/10.3389/fpls.2021.622062>.
- Chiang, K., Liu, H., Bock, C., 2017. A discussion on disease severity index values: warning on inherent errors and suggestions to maximize accuracy. *Ann. Appl. Biol.* 171, 139–154. <https://doi.org/10.1111/aab.12362>.
- Chithambarathanu, M., Jayakumar, M., 2023. Survey on crop pest detection using deep learning and machine learning approaches. *Multimed. Tools Appl.* 82, 42277–42310. <https://doi.org/10.1007/s11042-023-15221-3>.
- Colorado, J.D., Cera-Bornacelli, N., Caldas, J.S., Petro, E., Rebolledo, M.C., Cuellar, D., Calderon, F., Mondragon, I.F., Jaramillo-Butero, A., 2020. Estimation of nitrogen in rice crops from UAV-captured images. *Remote Sens.* 12. <https://doi.org/10.3390/rs12203396>.
- Danilevicius, M.F., Bayer, P.E., Boussaid, F., Bennamoun, M., Edwards, D., 2021. Maize yield prediction at an early developmental stage using multispectral images and genotype data for preliminary hybrid selection. *Remote Sens.* 13. <https://doi.org/10.3390/rs13193976>.
- DARPA, 2024. Shakey the Robot. darpa.mil/about-us/timeline/shakey-the-robot Accessed on August 9, 2023.
- Datta, D., Paul, M., Murshed, M., Teng, S.W., Schmidtke, L., 2023. Comparative analysis of machine and deep learning models for soil properties prediction from hyperspectral visual band. *Environments* 10. <https://doi.org/10.3390/environments10050077>.
- Edem Gold, 2023. The History of Artificial Intelligence from the 1950s to Today. <https://www.freecodecamp.org/news/the-history-of-ai/> Accessed on August 9, 2023.
- Elsayed, S., Elhoweity, M., Ibrahim, H.H., Dewir, Y.H., Migdadi, H.M., Schmidhalter, U., 2017. Thermal imaging and passive reflectance sensing to estimate the water status and grain yield of wheat under different irrigation regimes. *Agric. Water Manag.* 189, 98–110. <https://doi.org/10.1016/j.agwat.2017.05.001>.
- Elvanidi, A., Katsoulas, N., Kittas, C., 2018. Automation for water and nitrogen deficit stress detection in soilless tomato crops based on spectral indices. *Horticulturae* 4. <https://doi.org/10.3390/horticulturae4040047>.
- Esgario, J.G., Krohling, R.A., Ventura, J.A., 2020. Deep learning for classification and severity estimation of coffee leaf biotic stress. *Comput. Electron. Agric.* 169, 105162. <https://doi.org/10.1016/j.compag.2019.105162>.
- Espinoza, C.Z., Khot, L.R., Sankaran, S., Jacoby, P.W., 2017. High resolution multispectral and thermal remote sensing-based water stress assessment in subsurface irrigated grapevines. *Remote Sens.* 9. <https://doi.org/10.3390/rs9090961>.
- Essaadia, A., Abdellah, A., Ahmed, A., Abdelouahed, F., Kamal, E., 2022. The normalized difference vegetation index (ndvi) of the zat valley, Marrakech: comparison and dynamics. *Heliyon* 8, e12204. <https://doi.org/10.1016/j.heliyon.2022.e12204>.
- Farooque, A.A., Hussain, N., Schumann, A.W., Abbas, F., Afzaal, H., McKenzie-Gopsill, A., Esau, T., Zaman, Q., Wang, X., 2023. Field evaluation of a deep learning-based smart variable-rate sprayer for targeted application of agrochemicals. *Smart Agricult. Technol.* 3, 100073. <https://doi.org/10.1016/j.atech.2022.100073>.
- Fenu, G., Mallocci, F.M., 2021. Using multioutput learning to diagnose plant disease and stress severity. *Complexity* 2021 (6663442), 11. <https://doi.org/10.1155/2021/6663442>.
- Ford, T., Nagchaudhuri, A., Hartman, C., Mitra, M., 2019. Mission planning and orthomosaicking of uas imagery for remote sensing in precision agriculture on winter wheat and a subsurface drip irrigated (SDI) corn field. <https://doi.org/10.13031/aim.201900795>.
- Fraccaro, P., Butt, J., Edwards, B., Freckleton, R.P., Childs, D.Z., Reusch, K., Comont, D., 2022. A deep learning application to map weed spatial extent from unmanned aerial vehicles imagery. *Remote Sens.* 14. <https://doi.org/10.3390/rs14174197>.
- Friha, O., Ferrag, M.A., Shu, L., Maglaras, L., Wang, X., 2021. Internet of things for the future of smart agriculture: a comprehensive survey of emerging technologies. *IEEE/CAA J. Autom. Sinica* 8, 718–752. <https://doi.org/10.1109/JAS.2021.1003925>.
- Fu, Y., Yang, G., Pu, R., Li, Z., Li, H., Xu, X., Song, X., Yang, X., Zhao, C., 2021. An overview of crop nitrogen status assessment using hyperspectral remote sensing: current status and perspectives. *Eur. J. Agron.* 124, 126241. <https://doi.org/10.1016/j.eja.2021.126241>.
- Gabriels, S.H., Mishra, P., Mensink, M.G., Spoelstra, P., Woltering, E.J., 2020. Non-destructive measurement of internal browning in mangoes using visible and near-infrared spectroscopy supported by artificial neural network analysis. *Postharvest Biol. Technol.* 166, 111206. <https://doi.org/10.1016/j.postharvbio.2020.111206>.
- Gao, H., Huang, Z., Yang, H., Zhang, X., Cen, C., 2023. Research on improved multi-channel image stitching technology based on fast algorithms. *Electronics* 12. <https://doi.org/10.3390/electronics12071700>.
- García-Lara, S., Saldivar, S.S., 2016. Insect pests. In: Caballero, B., Finglas, P.M., Toldrá, F. (Eds.), *Encyclopedia of Food and Health*. Academic Press, Oxford, pp. 432–436. URL: <https://www.sciencedirect.com/science/article/pii/B9780123849472003962>. <https://doi.org/10.1016/B978-0-12-384947-2.00396-2>.
- Gioi, R., Jakubowicz, J., Morel, J.M., Randall, G., 2010. Lsd: a fast line segment detector with a false detection control. *IEEE Trans. Pattern Anal. Mach. Intell.* 32, 722–732. <https://doi.org/10.1109/TPAMI.2008.300>.
- Gitelson, A.A., 2004. Wide dynamic range vegetation index for remote quantification of biophysical characteristics of vegetation. *J. Plant Physiol.* 161, 165–173. <https://doi.org/10.1078/0176-1617-01176>.
- Gitelson, A.A., Kaufman, Y.J., Merzlyak, M.N., 1996. Use of a green channel in remote sensing of global vegetation from eos-modis. *Remote Sens. Environ.* 58, 289–298. [https://doi.org/10.1016/S0034-4257\(96\)00072-7](https://doi.org/10.1016/S0034-4257(96)00072-7).
- Gong, Y., Duan, B., Fang, S.E.A., 2018. Remote estimation of rapeseed yield with unmanned aerial vehicle (uav) imaging and spectral mixture analysis. *Plant Methods* 14, e12204. <https://doi.org/10.1186/s13007-018-0338-z>.
- Gonzalez-dugo, V., Zarco-Tejada, P., Nicolás, E., Nortes, P., Alarcón, J., Intrigliolo, D., Fereres, E., 2013. Using high resolution uav thermal imagery to assess the variability in the water status of five fruit tree species within a commercial orchard. *Precis. Agric.* 14. <https://doi.org/10.1007/s11119-013-9322-9>.
- Grgić, K., Žagar, D., Balen, J., Vlaović, J., 2020. Internet of things in smart agriculture – possibilities and challenges. 2020 International Conference on Smart Systems and Technologies (SST), pp. 239–244. <https://doi.org/10.1109/SST49455.2020.9264043>.
- Guevara, L., Hanheide, M., Parsons, S., 2021. Implementation of a humanaware robot navigation module for cooperative soft-fruit harvesting operations. *J. Field Robot.*, 1–31. <https://doi.org/10.1002/rob.22227>.
- Haboudane, D., Miller, J.R., Pattey, E., Zarco-Tejada, P.J., Strachan, I.B., 2004. Hyperspectral vegetation indices and novel algorithms for predicting green lai of crop canopies: modeling and validation in the context of precision agriculture. *Remote Sens. Environ.* 90, 337–352. <https://doi.org/10.1016/j.rse.2003.12.013>.
- Haider, T., Farid, M.S., Mahmood, R., Ilyas, A., Khan, M.H., Haider, S.T.A., Chaudhry, M.H., Gul, M., 2021. A computer-vision-based approach for nitrogen content estimation in plant leaves. *Agriculture* 11. <https://doi.org/10.3390/agriculture11080766>.
- Hassan, S.M., Maji, A.K., 2022. Plant disease identification using a novel convolutional neural network. *IEEE Access* 10, 5390–5401. <https://doi.org/10.1109/ACCESS.2022.3141371>.
- Hu, C., Thomasson, J.A., Bagavathiannan, M.V., 2021. A powerful image synthesis and semi-supervised learning pipeline for site-specific weed detection. *Comput. Electron. Agric.* 190, 106423. <https://doi.org/10.1016/j.compag.2021.106423>.
- Huang, H., Deng, J., Lan, Y., Yang, A., Deng, X., Wen, S., Zhang, H., Zhang, Y., 2018. Accurate weed mapping and prescription map generation based on fully convolutional networks using uav imagery. *Sensors* 18, 3299. <https://doi.org/10.3390/s18103299>.
- Huete, A., 1988. A soil-adjusted vegetation index (savi). 25 pp. 295–309.
- Huete, A., Didan, K., Miura, T., Rodriguez, E., Gao, X., Ferreira, L., 2002. Overview of the radiometric and biophysical performance of the modis vegetation indices. *Remote Sens. Environ.* 83, 195–213. [https://doi.org/10.1016/S0034-4257\(02\)00096-2](https://doi.org/10.1016/S0034-4257(02)00096-2).
- Huete, A., Didan, K., Van Leeuwen, W., Miura, T., Glenn, E., 2011. MODIS Vegetat. Indices 11, 579–602. https://doi.org/10.1007/978-1-4419-6749-7_26.
- IDB, 2023. Index database. A database for remote sensing indices. <https://www.indexdatabase.de/db/i.php?offset=1> Accessed: 05 July 2023.
- Ilyas, Q.M., Ahmad, M., Mehmood, A., 2023. Automated estimation of crop yield using artificial intelligence and remote sensing technologies. *Bioengineering* 10. <https://doi.org/10.3390/bioengineering10020125>.
- Integrated Drought Management Programme, 2024. Enhanced Vegetation Index (EVI). <https://www.droughtmanagement.info/enhancedvegetation-index-evi/> Accessed on July 21, 2023.
- Islam, M., Dinh, A., Wahid, K., Bhowmik, P., 2017. Detection of potato diseases using image segmentation and multiclass support vector machine. 2017 IEEE 30th Canadian Conference on Electrical and Computer Engineering (CCECE), pp. 1–4. <https://doi.org/10.1109/CCECE.2017.7946594>.
- Jackulin, C., Murugavalli, S., 2022. A comprehensive review on detection of plant disease using machine learning and deep learning approaches. *Measur. Sens.* 24, 100441. <https://doi.org/10.1016/j.measen.2022.100441>.
- Janani, A., Alboul, L., Penders, J., 2016. Multi robot cooperative area coverage, case study: Spraying. In: Alboul, L., Damian, D., Aitken, J.M. (Eds.), *Towards Autonomous Robotic Systems*. Springer International Publishing, Cham, pp. 165–176.
- Kakani, V., Nguyen, V.H., Kumar, B.P., Kim, H., Pasupuleti, V.R., 2020. A critical review on computer vision and artificial intelligence in food industry. *J. Agric. Food Res.* 2, 100033. <https://doi.org/10.1016/j.jafr.2020.100033>.
- Kamarudin, M., Ismail, Z.H., 2022. Lightweight deep CNN models for identifying drought stressed plant. *IOP Conference Series: Earth and Environmental Science*. 1091, p. 012043. <https://doi.org/10.1088/1755-1315/1091/1/012043>.
- Kestur, R., Meduri, A., Narasipura, O., 2019. Mangonet: a deep semantic segmentation architecture for a method to detect and count mangoes in an open orchard. *Eng. Appl. Artif. Intell.* 77, 59–69. <https://doi.org/10.1016/j.engappai.2018.09.011>.
- Khan, S., Tufail, M., Khan, M., Khan, Z., Iqbal, J., Wasim, A., 2021. Real-time recognition of spraying area for uav sprayers using a deep learning approach. *PLoS One* 16, e0249436. <https://doi.org/10.1371/journal.pone.0249436>.
- Kuzy, J., Jiang, Y., Li, C., 2018. Blueberry bruise detection by pulsed thermographic imaging. *Postharvest Biol. Technol.* 136, 166–177. <https://doi.org/10.1016/j.postharvbio.2017.10.011>.
- Lal, R., Sharda, A., Prabhakar, P., 2017. Optimal multi-robot path planning for pesticide spraying in agricultural fields. 2017 IEEE 56th Annual Conference on Decision and Control (CDC), pp. 5815–5820. <https://doi.org/10.1109/CDC.2017.8264538>.
- Lee, H., Lee, S., Choi, O., 2020. Improved method on image stitching based on optical flow algorithm. *Int. J. Eng. Business Manag.* 12. <https://doi.org/10.1177/1847979020980928>.

- Lee, J.H., Vo, H.T., Kwon, G.J., Kim, H.G., Kim, J.Y., 2023. Multicamera-based sorting system for surface defects of apples. *Sensors* 23. <https://doi.org/10.3390/s23083968>.
- Li, A., Zhou, S., Wang, R., 2017. An improved method for eliminating ghosting in image stitching. 2017 9th International Conference on Intelligent Human-Machine Systems and Cybernetics (IHMSC), pp. 415–418. <https://doi.org/10.1109/IHMSC.2017.205>.
- Li, H., Guo, C., Yang, Z., Chai, J., Shi, Y., Liu, J., Zhang, K., Liu, D., Xu, Y., 2022. Design of field real-time target spraying system based on improved yolov5. *Front. Plant Sci.* 13. <https://doi.org/10.3389/fpls.2022.1072631>.
- Li, J., Li, C., Luo, X., Chen, C.L.P., Chen, W., 2023. Realtime pineapple detection for agricultural robot via lightweight yolov7-tiny model. *Procedia Computer Science*, 226, pp. 92–98. <https://doi.org/10.1016/j.procs.2023.10.641> Proceedings of International Conference on Biomimetic Intelligence and Robotics.
- Liu, G.E.A., 2022. On the acquisition of high-quality digital images and extraction of effective color information for soil water content testing. *Sensors* 22, 3130. <https://doi.org/10.3390/s22093130>.
- Liu, J., Wang, X., 2021. Plant diseases and pests detection based on deep learning: a review. *Plant Methods* 17. <https://doi.org/10.1186/s13007-021-00722-9>.
- Liu, Y., He, M., Wang, Y., Sun, Y., Gao, X., 2022. Farmland aerial images faststitching method and application based on improved sift algorithm. *IEEE Access* 10, 95411–95424. <https://doi.org/10.1109/ACCESS.2022.3204657>.
- Liu, J., Jiang, W., Han, H., He, M., Gu, W., 2023. Satellite internet of things for smart agriculture applications: a case study of computer vision. 2023 20th Annual IEEE International Conference on Sensing, Communication, and Networking (SECON), pp. 66–71. <https://doi.org/10.1109/SECON58729.2023.10287508>.
- Lu, B., Dao, P.D., Liu, J., He, Y., Shang, J., 2020. Recent advances of hyperspectral imaging technology and applications in agriculture. *Remote Sens.* 12. <https://doi.org/10.3390/rs12162659>.
- Luo, J., Li, B., Leung, C., 2023. A survey of computer vision technologies in urban and controlled-environment agriculture. p. 56. <https://doi.org/10.1145/3626186>.
- Maheswari, P., Raja, P., Hoang, V., 2022. Intelligent yield estimation for tomato crop using segnet with vgg19 architecture. *Sci. Rep.* 12. <https://doi.org/10.1038/s41598-022-17840-6>.
- Maresma, Ariza M., Martínez, E., Lloveras, J., Martínez-Casasnovas, J.A., 2016. Analysis of vegetation indices to determine nitrogen application and yield prediction in maize (zea mays l.) from a standard uav service. *Remote Sens.* 8. <https://doi.org/10.3390/rs8120973>.
- Marin, D.B., e Silva Ferraz, G.A., Santana, L.S., Barbosa, B.D.S., Barata, R.A.P., Osco, L.P., Ramos, A.P.M., Guimarães, P.H.S., 2021. Detecting coffee leaf rust with uav-based vegetation indices and decision tree machine learning models. *Comput. Electron. Agric.* 190, 106476. <https://doi.org/10.1016/j.compag.2021.106476>.
- Marks, J., 2023. How computer vision is changing agriculture in 2023. <https://voxel51.com/blog/how-computer-vision-is-changing-agriculture-in-2023/> Accessed: 22 April 2023.
- Masdani, M., Darlis, D., 2018. A comprehensive study on mqtt as a low power protocol for internet of things application. *IOP Conf. Ser. Mater. Sci. Eng.* 434, 012274. <https://doi.org/10.1088/1757-899X/434/1/012274>.
- Megha, V., Rajkumar, K.K., 2022. A comparative study on different image stitching techniques. *Int. J. Eng. Trends Technol.* 70, 44–58. <https://doi.org/10.14445/22315381/IJETT-V70I4P205>.
- Mehrish, R., Pemeena Priyadarsini, J., Murugesan, K., Inabathini, S., Jabeena, A., Senthil, R., 2014. Comprehensive analysis and efficiency comparison of image stitching techniques. *ARPN J. Eng. Appl. Sci.* 9, 935–952.
- Melesse, T.Y., Bollo, M., Pasquale, V.D., Centro, F., Riemma, S., 2022. Machine learning-based digital twin for monitoring fruit quality evolution. *Procedia Comp. Sci.* 200, 13–20. <https://doi.org/10.1016/j.procs.2022.01.200>. (3rd International Conference on Industry 4.0 and Smart Manufacturing).
- Merzlyak, M.N., Gitelson, A.A., Chivkunova, O.B., Rakin, V.Y., 1999. Non-destructive optical detection of pigment changes during leaf senescence and fruit ripening. *Physiol. Plant.* 106, 135–141. <https://doi.org/10.1034/j.1399-3054.1999.106119.x>.
- Mesas-Carrascosa, F.J., Rumbao, I.C., Torres-Sánchez, J., García-Ferrer, A., Peña, J.M., Granados, E.L., 2017. Accurate ortho-mosaicked six-band multispectral uav images as affected by mission planning for precision agriculture proposes. *Int. J. Remote Sens.* 38, 2161–2176. <https://doi.org/10.1080/01431161.2016.1249311>.
- Moghadam, P., Ward, D., Goan, E., Jayawardena, S., Sikka, P., Hernandez, E., 2017. Plant disease detection using hyperspectral imaging. 2017 International Conference on Digital Image Computing: Techniques and Applications (DICTA), pp. 1–8. <https://doi.org/10.1109/DICTA.2017.8227476>.
- Munir, A., Blasch, E., Kwon, J., Kong, J., Aved, A., 2021. Artificial intelligence and data fusion at the edge. *IEEE Aerosp. Electron. Syst. Mag.* 36, 62–78.
- Munir, A., Kong, J., Qureshi, M.A., 2024. *Accelerators for Convolutional Neural Networks*. Wiley-IEEE Press.
- Mwinuka, P.R., Mourice, S.K., Mbungu, W.B., Mbilinyi, B.P., Tumbo, S.D., Schmitter, P., 2022. Uav-based multispectral vegetation indices for assessing the interactive effects of water and nitrogen in irrigated horticultural crops production under tropical humid conditions: a case of african eggplant. *Agric. Water Manag.* 266, 107516. <https://doi.org/10.1016/j.agwat.2022.107516>.
- NDWI – EUROPE, P.F.S., 2011. NDWI: Normalized difference water index. https://edo.jrc.ec.europa.eu/documents/factsheets/factsheet_ndwi.pdf Accessed: 20 July 2023.
- Nturambirwe, J.F.I., Opara, U.L., 2020. Machine learning applications to nondestructive defect detection in horticultural products. *Biosyst. Eng.* 189, 60–83. <https://doi.org/10.1016/j.biosystemseng.2019.11.011>.
- Ouhami, M., Hafiane, A., Es-Saady, Y., El Hajji, M., Canals, R., 2021. Computer vision, iot and data fusion for crop disease detection using machine learning: a survey and ongoing research. *Remote Sens.* 13. <https://doi.org/10.3390/rs13132486>.
- Patrício, D.I., Rieder, R., 2018. Computer vision and artificial intelligence in precision agriculture for grain crops: a systematic review. *Comput. Electron. Agric.* 153, 69–81. <https://doi.org/10.1016/j.compag.2018.08.001>.
- Pix4D, 2021. Photo stitching vs orthomosaic generation. <https://support.pix4d.com/hc/en-us/articles/202558869-Photostitching-vs-orthomosaic-generation> Accessed: 02 April 2023.
- Pretto, A., Aravecchia, S., Burgard, W., Chebrolu, N., Dornhege, C., Falck, T., Fleckenstein, F., Fontenla, A., Imperoli, M., Khanna, R., Liebisch, F., Lottes, P., Milioto, A., Nardi, D., Nardi, S., Pfeifer, J., Popović, M., Potena, C., Pradalier, C., Rothacker-Feder, E., Sa, I., Schaefer, A., Siegwart, R., Stachniss, C., Walter, A., Winterhalter, W., Wu, X., Nieto, J., 2021. Building an aerial-ground robotics system for precision farming: An adaptable solution. *IEEE Robot. Autom. Mag.* 28, 29–49. <https://doi.org/10.1109/MRA.2020.3012492>.
- Qiao, M., He, X., Cheng, X., Li, P., Luo, H., Zhang, L., Tian, Z., 2021. Crop yield prediction from multi-spectral, multi-temporal remotely sensed imagery using recurrent 3d convolutional neural networks. *Int. J. Appl. Earth Obs. Geoinf.* 102, 102436. <https://doi.org/10.1016/j.jag.2021.102436>.
- Qin, F., Liu, D., Sun, B., Ruan, L., Ma, Z., Wang, H., 2016. Identification of alfalfa leaf diseases using image recognition technology. p. 11.
- Quebrajo, L., Perez-Ruiz, M., Pérez-Urrestarazu, L., Martínez, G., Egea, G., 2018. Linking thermal imaging and soil remote sensing to enhance irrigation management of sugar beet. *Biosyst. Eng.* 165, 77–87. <https://doi.org/10.1016/j.biosystemseng.2017.08.013> Sensing and Control of Crop Water Status.
- Ramya, C.M., Shanmugaraj, M., Prabakaran, R., 2011. Study on zigbee technology. 2011 3rd International Conference on Electronics Computer Technology, pp. 297–301. <https://doi.org/10.1109/ICECTECH.2011.5942102>.
- Roldán, J.J., García-Aunon, P., Garzón, M., De León, J., Del Cerro, J., Barrien Tos, A., 2016. Heterogeneous multi-robot system for mapping environmental variables of greenhouses. *Sensors* 16. <https://doi.org/10.3390/s16071018>.
- Rondeaux, G., 1996. Optimization of soil-adjusted vegetation indices. 55 pp. 95–107.
- Roujean, J.L., Breon, F.M., 1995. Estimating par absorbed by vegetation from bidirectional reflectance measurements. *IFAC Proc.* 51, 375–384. [https://doi.org/10.1016/0034-4257\(94\)00114-3](https://doi.org/10.1016/0034-4257(94)00114-3).
- Rubo, S., Zinkernagel, J., 2022. Exploring hyperspectral reflectance indices for the estimation of water and nitrogen status of spinach. *Biosyst. Eng.* 214, 58–71. <https://doi.org/10.1016/j.biosystemseng.2021.12.008>.
- Sabah, N., Usama, M., Zafar, Z., Shahzad, M., Fraz, M., Berns, K., 2022. Analysis of vegetation indices in the cotton crop in south asia region using uav imagery. , pp. 70–75. <https://doi.org/10.1109/ICET56601.2022.10004662>.
- Saleem, M.H., Potgieter, J., Arif, K.M., 2022. A performance-optimized deep learning-based plant disease detection approach for horticultural crops of New Zealand. *IEEE Access* 10, 89798–89822. <https://doi.org/10.1109/ACCESS.2022.3201104>.
- Santos Pereira, L.F., Barbon, S., Valous, N.A., Barbin, D.F., 2018. Predicting the ripening of papaya fruit with digital imaging and random forests. *Comput. Electron. Agric.* 145, 76–82. <https://doi.org/10.1016/j.compag.2017.12.029>.
- Sethy, P.K., Pandey, C., Sahu, Y.K., Behera, S.K., 2022. Hyperspectral imagery applications for precision agriculture - a systemic survey. *Multimed. Tools Appl.* 81, 3005–3038. <https://doi.org/10.1007/s11042-021-11729-8>.
- Seyyedhasani, H., Peng, C., Jiunn Jang, W., Vougioukas, S.G., 2020. Collaboration of human pickers and crop-transporting robots during harvesting – Part I: Model and simulator development. *Comput. Electron. Agric.* 172, 105324. <https://doi.org/10.1016/j.compag.2020.105324>.
- Shafik, W., Tufail, A., Namoun, A., De Silva, L.C., Apong, R.A.A.H.M., 2023. A systematic literature review on plant disease detection: motivations, classification techniques, datasets, challenges, and future trends. *IEEE Access* 11, 59174–59203. <https://doi.org/10.1109/ACCESS.2023.3284760>.
- Shahi, T.B.E.A., 2023. A cooperative scheme for late leaf spot estimation in peanut using uav multispectral images. *PLoS One* 18, e0282486. <https://doi.org/10.1371/journal.pone.0282486>.
- Singh, A., Gaurav, K., 2023. Deep learning and data fusion to estimate surface soil moisture from multi-sensor satellite images. *Sci. Rep.* 13, 2251. <https://doi.org/10.1038/s41598-023-28939-9>.
- Sudarsan, B., Ji, W., Biswas, A., Adamchuk, V., 2016. Microscope-based computer vision to characterize soil texture and soil organic matter. *Biosyst. Eng.* 152, 41–50. <https://doi.org/10.1016/j.biosystemseng.2016.06.006>.
- Tagarakis, A.C., Filippou, E., Kalaitzidis, D., Benos, L., Busato, P., Bochtis, D., 2022. Proposing ugv and uav systems for 3d mapping of orchard environments. *Sensors* 22. <https://doi.org/10.3390/s22041571>.
- Tang, J., Arvor, D., Corpetti, T., Tang, P., 2021. Mapping center pivot irrigation systems in the southern amazon from sentinel-2 images. *Water* 13. <https://doi.org/10.3390/w13030298>.
- Tang, W., Jia, F., Wang, X., 2023. An improved adaptive triangular mesh-based image warping method. *Front. Neurobot.* 16. <https://doi.org/10.3389/fnbot.2022.1042429>.
- Tariq, M.A., Khan, M., Raza Khan, M.T., Kim, D., 2020. Enhancements and challenges in coap—a survey. *Sensors*, 20. <https://doi.org/10.3390/s20216391>. URL <https://www.mdpi.com/1424-8220/20/21/6391>.
- Théau, J., Gavelle, E., Ménard, P., 2020. Crop scouting using uav imagery: a case study for potatoes. *J. Unmanned Vehicle Syst.* 8, 99–118. <https://doi.org/10.1139/juvs-2019-0009>.
- Thorat, T., Patle, B., Kashyap, S.K., 2023. Intelligent insecticide and fertilizer recommendation system based on tfp-cnn for smart farming. *Smart Agricult. Technol.* 3, 100114. <https://doi.org/10.1016/j.atech.2022.100114>.
- Tian, H., Wang, T., Liu, Y., Qiao, X., Li, Y., 2020. Computer vision technology in agricultural automation — a review. *Inform. Proces. Agric.* 7, 1–19. <https://doi.org/10.1016/j.inpa.2019.09.006>.

- Ullo, S.L., Sinha, G.R., 2021. Advances in iot and smart sensors for remote sensing and agriculture applications. *Remote Sens.* 13. <https://doi.org/10.3390/rs13132585>.
- USDA, 2023. Normalized Difference Vegetation Index (NDVI). <https://ipad.fas.usda.gov/cropexplorer/Definitions/spotveg.htm> Accessed on July 18, 2023.
- van Klompenburg, T., Kassahun, A., Catal, C., 2020. Crop yield prediction using machine learning: a systematic literature review. *Comput. Electron. Agric.* 177, 105709. <https://doi.org/10.1016/j.compag.2020.105709>.
- Vásconez Hurtado, J., Kantor, G., Auat Cheein, F., 2019. Human–robot interaction in agriculture: a survey and current challenges. *Biosyst. Eng.* 179, 35–48. <https://doi.org/10.1016/j.biosystemseng.2018.12.005>.
- Wagner, D., Munir, A., Neilsen, M., 2021. A novel system architecture for automated field-based tent systems for controlled-environment agriculture. 2021 IEEE International Symposium on Smart Electronic Systems (iSES), pp. 105–110. <https://doi.org/10.1109/iSES52644.2021.00034>.
- WUR, 2017. Smart colour inspector - Agri food colour measurement instrument. <https://www.wur.nl/en/project/Smart-Colour-Inspector-agri-food-colour-measurement-instrument.htm> Accessed: 02 June 2023.
- Yang, C., Feng, M., Song, L.E.A., 2021a. Study on hyperspectral estimation model of soil organic carbon content in the wheat field under different water treatments. *Sci. Rep.* 11. <https://doi.org/10.1038/s41598-021-98143-0>.
- Yang, X., Bao, N., Li, W., Liu, S., Fu, Y., Mao, Y., 2021b. Soil nutrient estimation and mapping in farmland based on UAV imaging spectrometry. *Sensors* 21. <https://doi.org/10.3390/s21113919> URL: <https://www.mdpi.com/1424-8220/21/11/3919>.
- Yu, K., Anderegg, J., Mikaberidze, A., Karisto, P., Mascher, F., McDonald, B.A., Walter, A., Hund, A., 2018. Hyperspectral canopy sensing of wheat septoria tritici blotch disease. *Front. Plant Sci.* 9. <https://doi.org/10.3389/fpls.2018.01195>.
- Yu, Q., Wang, R., Liu, F., Xiao, J., An, J., Liu, J., 2023. High precision meshbased drone image stitching based on salient structure preservation and regular boundaries. *Drones* 7. <https://doi.org/10.3390/drones7040230>.
- Yuan, Y., Fang, F., Zhang, G., 2021. Superpixel-based seamless image stitching for uav images. *IEEE Trans. Geosci. Remote Sens.* 59, 1565–1576. <https://doi.org/10.1109/TGRS.2020.2999404>.
- Zhang, C., Noguchi, N., 2017. Development of a multi-robot tractor system for agriculture field work. *Comput. Electron. Agric.* 142, 79–90. <https://doi.org/10.1016/j.compag.2017.08.017>.
- Zhang, P., Zhou, X.X., Wang, Z.E.A., 2020. Using hj-ccd image and pls algorithm to estimate the yield of field-grown winter wheat. *Sci. Rep.* 10. <https://doi.org/10.1038/s41598-020-62125-5>.
- Zhang, Z., Qiao, Y., Guo, Y., He, D., 2022. Deep learning based automatic grape downy mildew detection. *Front. Plant Sci.* 13, 872107. <https://doi.org/10.3389/fpls.2022.872107>.
- Zhao, H., Yang, C., Guo, W., Zhang, L., Zhang, D., 2020a. Automatic estimation of crop disease severity levels based on vegetation index normalization. *Remote Sens.* 12. <https://doi.org/10.3390/rs12121930>.
- Zhao, Y., Cheng, Y., Zhang, X., Xu, S., Bu, S., Jiang, H., Han, P., Li, K., Wan, G., 2020b. Real-time orthophoto mosaicing on mobile devices for sequential aerial images with low overlap. *Remote Sens.* 12. <https://doi.org/10.3390/rs12223739>.
- Zhao, B., Zhang, Y., Duan, A., Liu, Z., Xiao, J., Liu, Z., Qin, A., Ning, D., Li, S., Ata-Ul-Karim, S.T., 2021. Estimating the growth indices and nitrogen status based on color digital image analysis during early growth period of winter wheat. *Front. Plant Sci.* 12. <https://doi.org/10.3389/fpls.2021.619522>.